energies

Article

# Energy Savings in Elevators by Using a Particular Permanent-Magnet Motor Drive †

**Vasileios I. Vlachou [1], Theoklitos S. Karakatsanis [2] and Antonios G. Kladas [1,*]**

[1] Laboratory of Electrical Machines and Power Electronics, Department of Electrical and Computer Engineering, National Technical University of Athens, 15780 Athens, Greece; vasilvlachou@mail.ntua.gr
[2] Laboratory of Thermodynamics and Thermal Machines, Department of Production and Management Engineering, Democritus University of Thrace, 67100 Xanthi, Greece; thkarak@pme.duth.gr
* Correspondence: kladasel@central.ntua.gr; Tel.: +30-210-7723-765
† This paper is an extended version of our paper published in 13th Mediterranean Conference on Power Generation, Transmission, Distribution and Energy Conversion (MEDPOWER).

**Abstract:** This paper presents the energy savings achieved by using a particular three-phase permanent-magnet motor drive control strategy in an elevator application. The proposed control methodology, based on a particular variable-amplitude variable-frequency voltage control pattern technique implemented in a permanent-magnet motor, is compared to a standard induction motor elevator case. By adopting appropriate simultaneous changes in the amplitude and frequency of the motor voltage, high speeds can be attained in conjunction with smooth starting and stopping actions involving a reduced supply current during the respective movement of the elevator. In addition, this method exhibits a high power factor with a good driving quality. The control technique introduced achieves the levelling-off of the floor and the group movement of the system using in the programmable memory a speed pattern that is generated targeting proportionality to the position of the lift. In that respect, significant energy savings can be obtained, which, depending on the type of motor implemented, can be up to 30% compared to the conventional techniques. These improvements can be attained with the appropriate handling of the applied pulse width modulation techniques. Various simulated and experimental results are given, illustrating the respective energy savings achieved with the proposed methodology.

**Keywords:** electric drive; elevator; energy savings; permanent-magnet motor; variable-voltage variable-frequency; induction motor; sinusoidal pulse width modulation; counterweight



**Citation:** Vlachou, V.I.; Karakatsanis, T.S.; Kladas, A.G. Energy Savings in Elevators by Using a Particular Permanent-Magnet Motor Drive. *Energies* **2023**, *16*, 4716. https://doi.org/10.3390/en16124716

Academic Editors: Brian Azzopardi, Cyril Spiteri Staines, Saeed Golestan and Frede Blaabjerg

Received: 27 March 2023
Revised: 24 May 2023
Accepted: 9 June 2023
Published: 14 June 2023



## 1. Introduction

Electromobility is a very considerably growing technology due to its promising advantage of friendliness to the environment, expanding to a wide range of applications. Electric motors are used in a multitude of research areas with impacts on many applications in everyday life, such as electric vehicles and elevators [1,2].

Since elevators are intended for variable loading conditions and constitute very diverse applications, it is feasible, in addition to the appropriate selection of a suitable electric motor, to emphasize the motor-control strategy to be adopted, enabling the maximization of the percentage of energy savings that can be achieved [3]. In general, such applications use permanent-magnet motors to achieve a better performance, reaching efficiencies of up to 99% in several cases, involving a low maintenance cost as well as reduced volume and mass [4]. In the respective drive systems, there are different types of control techniques that can be adopted. The simpler and more easily implemented is the scalar control technique, targeting a specific steady-state operating point, while vector control methodologies enable transient operation optimization at the expense of additional complexity and cost. Due to the decoupled torque and flux connection, it operates just like a DC motor [5,6].

As motor drive systems tend to dominate in elevator applications, enabling important energy savings with respect to direct motor supply by the grid, the requirement of an appropriate power electronics converter is usually referred to as a variable-voltage variable-frequency (VVVF) inverter [7]. This control technique is used in simulations where greater energy savings are required each time the load torque is reduced while controlling the speed of the system [8].

Gradual control is one of the most popular strategies implemented in elevators due to its simple and easy implementation presenting important advantages with respect to a direct supply from the grid, especially in the medium- and higher-speed ranges. This method achieves control of the speed of the electrical motor through appropriately setting the ratio of the amplitude and the frequency of the supply voltage by conveniently monitoring the current. This control technique can be used in variable-speed applications, in particular when there are no special requirements regarding the dynamic response of the system [9]. Moreover, one of the main advantages of this control method is that it can be implemented without position sensors, but with restrictions to maintain the constant load [10]. The control technique adopted in this paper is a particular gradual control procedure based on a specific loading pattern.

## 2. Drive System Control

In order to achieve the drive system targets, shown in Figure 1, it is necessary to introduce an adequate control type involving convenient regulators. The current-, speed- and position-control procedures usually implement appropriate PI or PID controllers with application-based parameter tuning, enabling the tracking of constantly updated requirements of the driving system by means of convenient voltage-supply changes to the motor by the inverter [11]. In order to study the overall system's transient characteristics, it is useful to analyze the specific steady-state target operating conditions in a first step and then investigate the dynamic behavior of the various subsystems in a second step [12].

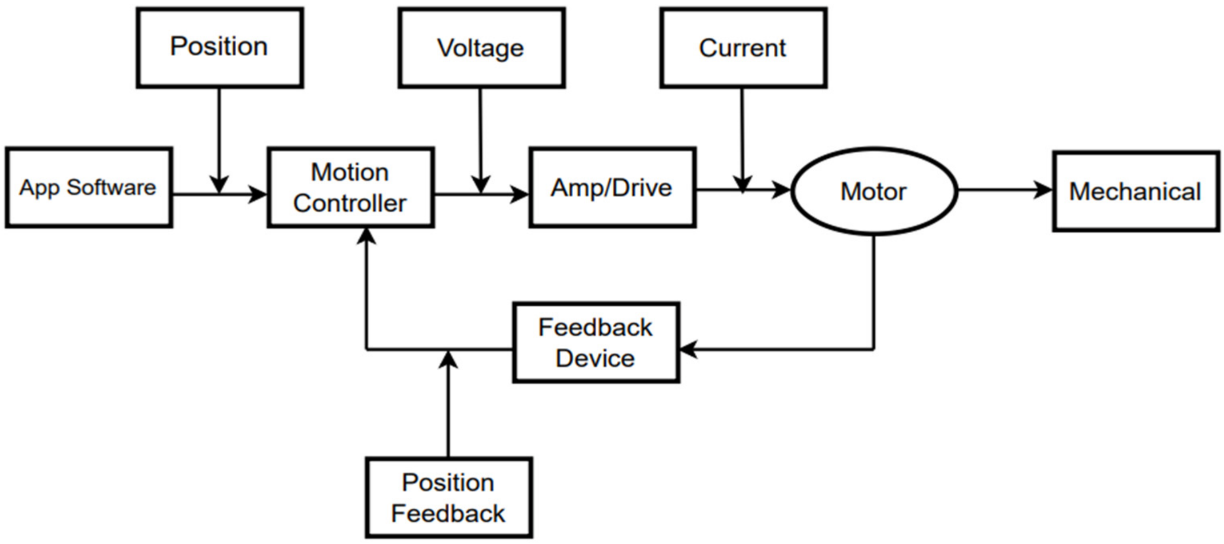


**Figure 1.** Block diagram of the basic motion system.

## 3. Vector Control of PMSM

The efficient operation of permanent-magnet synchronous motors (PMSM) necessitates the adoption of relatively demanding control techniques. Several different control strategies have already been developed for driving electric motors depending on the particular motor type and required operating characteristics. Such techniques present relative advantages and disadvantages, depending on the application considered [13]. Scalar control procedures, which are relatively simple and easily implemented, developed for induction motor drives, cannot be properly extended to permanent-magnet motor drives.

Vector control strategies, in contrast, were developed initially in induction motor drive cases for the efficient handling of transient operations at the expense of more complex hardware and implementation and are convenient for synchronous permanent-magnet drive applications, as can be seen from Figure 2a. Through these techniques, the stator currents are controlled by using a representation through a convenient vector corresponding to the resulting magneto-motive force in the air gap.

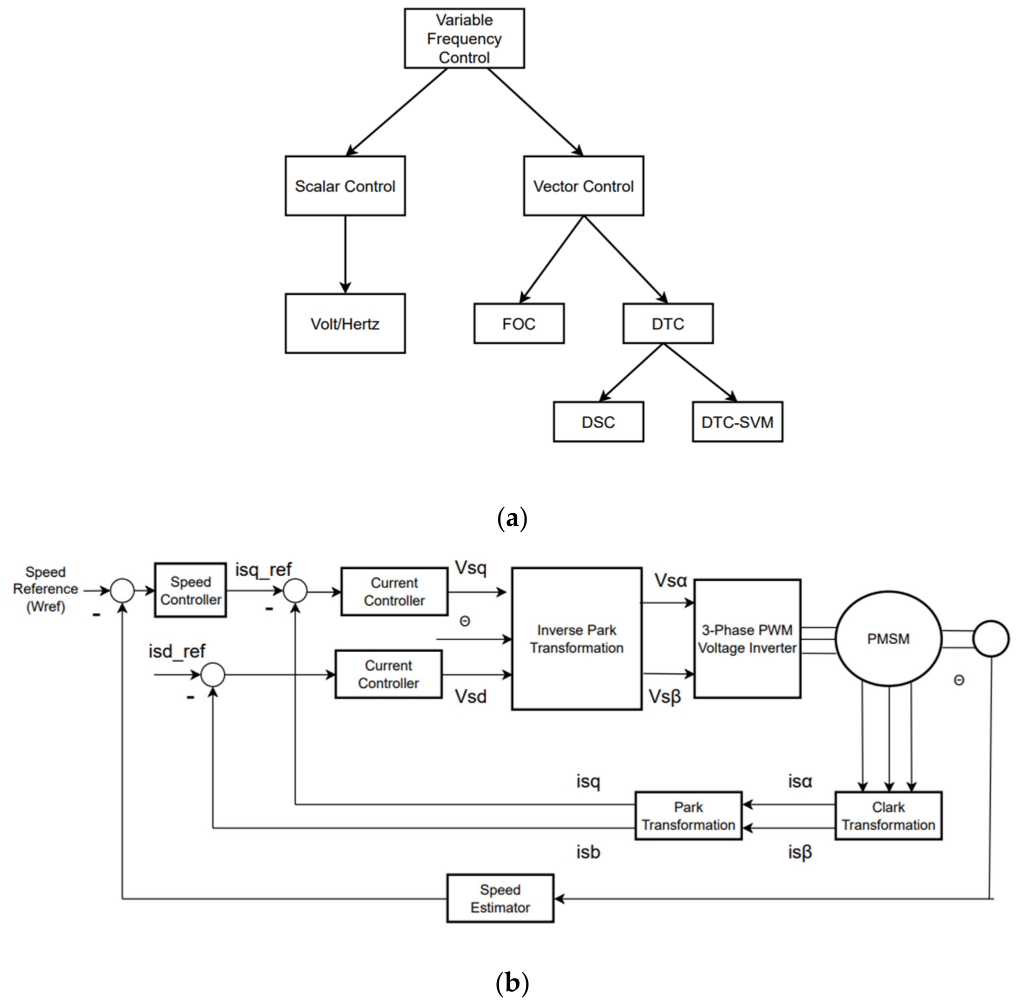


**Figure 2.** (**a**) AC motor control technique; (**b**) PMSM vector control drive system.

In particular, the stator currents are decomposed into two principal components along the direct (d) and quadrature (q) axes, respectively, through Park transformation in a rotating frame with the speed of magnetic field rotation. The d-axis current component is aligned with the rotor excitation in synchronous machines and controls the excitation flux, while the d-axis component is aligned along a vertical axis to the excitation and controls the electromagnetic torque of the motor, as shown in Figure 2b [14]. The main advantages of the vector control techniques over the scalar (usually designated as v/f) control techniques concern the transient operation and involve both motor efficiency and improved torque response as well as better torque control and speed adjustment at low speeds [15]. These advantages are of great importance in elevator applications and justify the required complexity of vector control. More specifically, it is necessary to accurately control the torque of the electrical motor, especially during landing of the car, as it can cause a speed error causing inaccuracies in the landing level and endangering the safety of the passengers. For the appropriate setting of the PI speed and current controllers use the corresponding standard in Table 1.

**Table 1.** Controller equations for the driving PMSM.

| Types of Controllers | Symbols | Equations |
|---|---|---|
| Current along d-axis (P) | $K_{pd}$ | $a_c L_d$ |
| Current along d-axis (I) | $K_{id}$ | $a_c{}^2 L_d$ |
| Current along q-axis (P) | $K_{pq}$ | $a_c L_q$ |
| Current along q-axis (I) | $K_{iq}$ | $a_c{}^2 L_q$ |
| Current controller bandwidth | $a_c$ | $\leq 0.04\ w_s$ |
| Analog speed controller gain (P) | $K_{ps}$ | $a_s \mathrm{J} \frac{4}{3P p_m}$ |
| Integral speed controller gain (I) | $K_{is}$ | $a_s \mathrm{B} \frac{4}{3P p_m}$ |
| Speed controller bandwidth | $a_s$ | $\leq 0.1\ w_c$ |

## 4. Structure of the Elevator Velocity-Control System

The evolution of power electronics has resulted in considerable improvements in elevator applications, such as continuous speed control by varying the frequency of the supplied current of the three-phase motor using a suitable inverter. The change in frequency enables fast changes in elevator speed, improving at the same time the efficiency under transients and achieving an optimal acceleration and deceleration. In high-speed ranges in particular, VVVF technology is very widely used and presents important advantages that save both energy and motor life [16]. The basic parts of a typical inverter implemented in elevator speed-control systems are the rectifier, the inverter and the control unit [17].

- Rectifier: The rectifier is the device that converts the three-phase alternating current of the network into direct current (AC/DC). It consists of the simple rectifying bridge and a smoothing filter comprising a capacitor and a coil [18].
- Inverter: The smoothed DC voltage then feeds the inverter. The purpose of the device is to convert the DC voltage into an AC of variable frequency and controlled amplitude. The basic building blocks of the inverter are electronic semiconductor power switches. The choice of these switches is very important and has a decisive influence on the operating characteristics, performance and also the quality of the inverter.
- Control Unit: The control unit is available to formulate a pulse width range of suitable amplitude. In order to achieve control of the fundamental harmonic of the inverter output voltage, it is necessary to vary the pulse width by varying the time intervals where the semiconductor elements are turned on or off. In general, the DC voltage of the inverter is converted into an alternating voltage with a controlled amplitude and frequency. In this way, each pulse is converted into a numerical bit from where it expresses the opening and closing of the three-phase inverter switches (on, off) [19].

The VVVF inverter, using appropriate microprocessors, has led to the development of multiple systems that run complex operating programs with an increased degree of control accuracy, providing improved reliability and flexibility. By varying the frequency of the supply voltage, the speed of the electrical motor can be adjusted over a wide range of elevator operations. With the development of power electronics and the use of appropriate control techniques in the inverters, it is possible to make the variation in frequency match the possibility of varying the supply voltage. In this way, the magnetic flux in the gap is maintained at its maximum. In normal operating conditions, we observe that the voltage drop of the stator winding is less than that of the stator anti-electromotive force ($I_a(R_1 + \mathrm{j}X_1) < E_1$) and results the following equation:

$$V_1 \approx 4.44 K_1 f_1 N_1 p_m \quad (1)$$

Based on Equation (1), we find that the flow in the gap is defined by the ratio $V_1/f_1 = V_{nom}/f_{nom}$. Observing Figure 3a,b according to the push-turn speed curves, we find that the maximum thrust decreases at low operating frequencies (less than 10 Hz). The effect of this decrease is due to the reduction in the magnetic flux in the gap, due to resistance of the stator winding. At low frequencies, the voltage drops across the $R_1$

winding resistance becomes comparable to the induced anti-electromotive force, so that the V/f ratio no longer applies and an additional voltage increase is required to maintain the magnetic flux at the desired amount to avoid overheating problems and operation at saturation conditions.

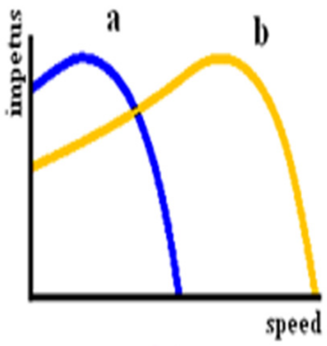


**Figure 3.** Characteristics of impetus speed. (**a**) Half of nominal voltage and frequency operation (blue); (**b**) nominal voltage and frequency operation (yellow).

In traction systems, increasing the starting thrust combined with reducing the frequency produces suitable results. Rotation control can be extended to frequencies greater than 50 Hz where the curves have the same shape but move to the right. In this case, for frequencies greater than 20 Hz the voltage drop of the stator winding can be ignored. Therefore, the operation of the electrical motor under steady state depends solely on the rotor frequency, so the characteristic speed curves have the same shape in this region.

In Figure 4a,b, showing the voltage pulses produced using a sinusoidal pulse width modulation (SPWM) technique, two cases are distinguished: (a) the modulation of the pulses in the case of half the nominal voltage and frequency and (b) the corresponding modulation of the pulses in the case of the nominal voltage and frequency depending on the programmed velocity and starting impetus.

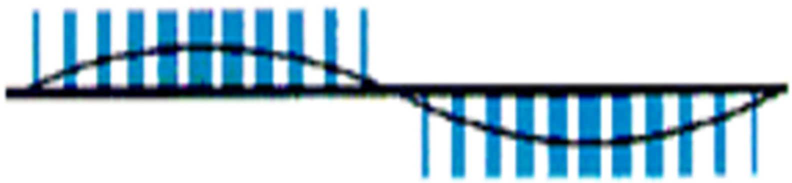

(**a**)

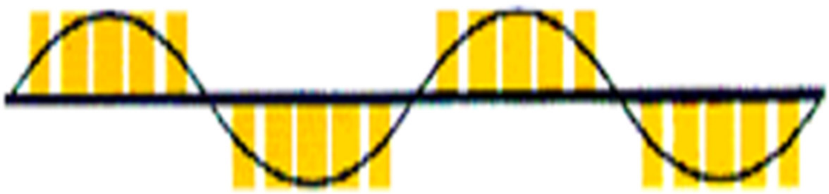

(**b**)

**Figure 4.** (**a**) Half of nominal voltage and frequency operation (blue); (**b**) nominal voltage and frequency operation (yellow).

As discussed above, there are various control techniques for successfully controlling and driving a permanent-magnet synchronous motor. Therefore, it is appropriate to use a suitable inverter with a suitable pulse width modulation. The most common pulse width modulation is sinusoidal pulse width modulation. A sine-wave reference signal is compared to a triangular carrier signal [20]. The IGBT are property-controlled with a series of ON–OFF pulses. Thus, in this way a DC voltage can give, with the appropriate technique, an alternating voltage at the output of the inverter with an increased fundamental component. In addition, no particular switching losses are observed, which has a result of eliminating the lower harmonics, so the PMSM has a higher performance [21]. Equations (1) and (2) relate to the amplitude modulation $M_a$ and frequency modulation $M_f$:

$$M_a = \frac{A_r}{A_c} \tag{2}$$

$$M_f = \frac{f_s}{f_c} \tag{3}$$

where $A_r$ is the amplitude of the reference waveform, $A_c$ is the amplitude of the triangular carrier waveform, $f_s$ is the frequency of the reference waveform and $f_c$ is the frequency of the triangular carrier waveform. The frequency ratio $M_f$ shows the number of pulses in the positive period and the number in the negative period.

## 5. Operation of VVVF Inverter Control

Figure 5a–d show the motion curves of the elevator during ascent and descent that should be followed in cases of empty load (0 kg), of half the nominal load (300 kg) and of full load (615 kg). The specific speed curves are programmed into the inverter to determine the movement of the system during elevator operation. These figures illustrate a typical elevator drive system target. Initially, it may be observed that when the cabin starts to move, it performs an acceleration motion period, while at the end of the trajectory the elevator comes to a standstill. However, before it enters the stall process, it must reduce its speed in order to safely perform the transition to the call floor. Based on the specific characteristic's curves, useful information can be derived concerning the time interval of each movement and the corresponding power consumed throughout the range of the movement.

Taking into account the time intervals of speed variation from the experimental velocity curves of the elevator depicted in Figure 5a,b and considering that the average speed is 1 m/s, the respective speed variation characteristics can be evaluated, which correspond to 0.4 m/s$^2$ of average acceleration and 0.35 m/s$^2$ of average deceleration. Based on the lift curve in Figure 5c,d we see that although the deceleration is much steeper the delay before stopping is longer.

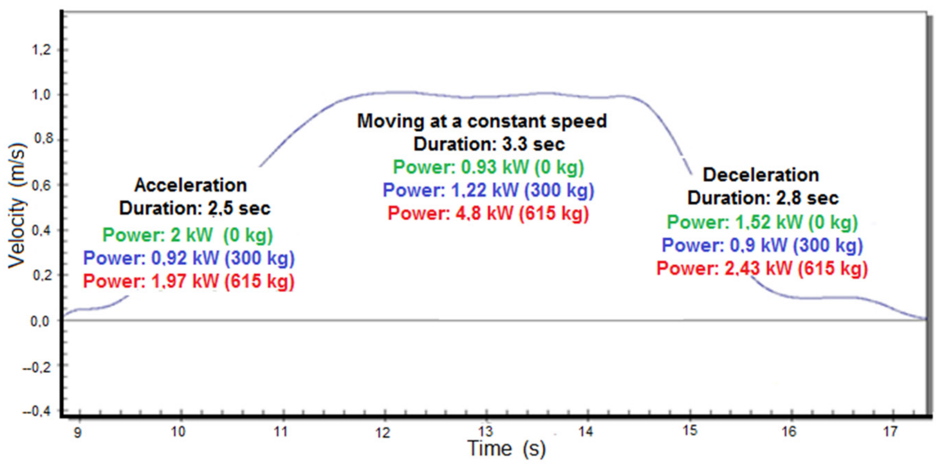


(**a**)

**Figure 5.** *Cont.*

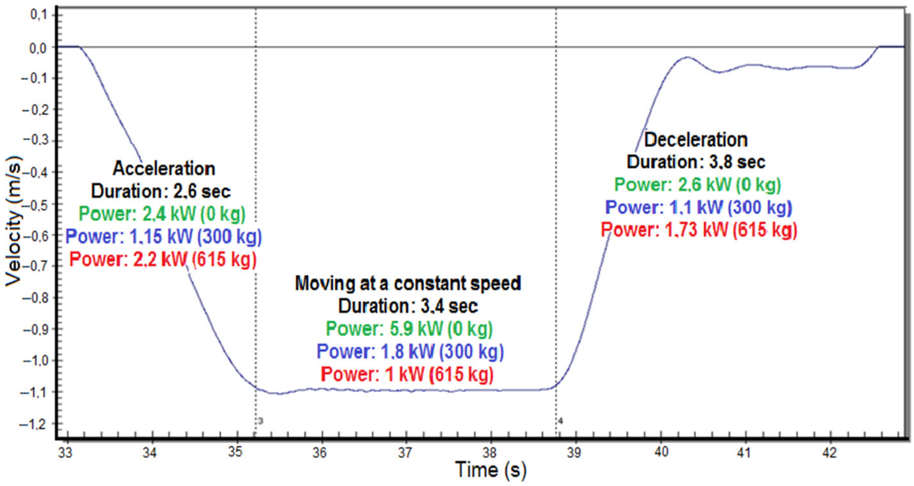


(**b**)

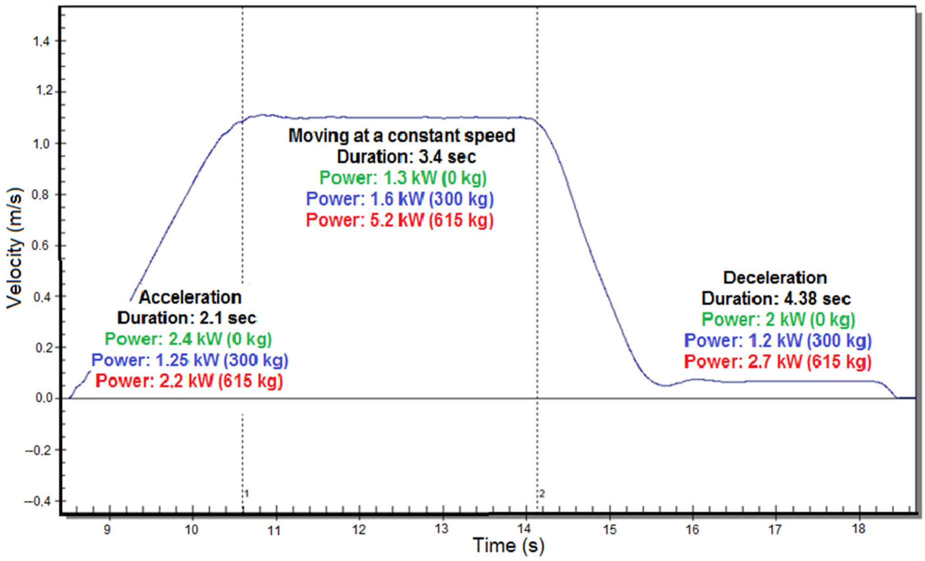


(**c**)

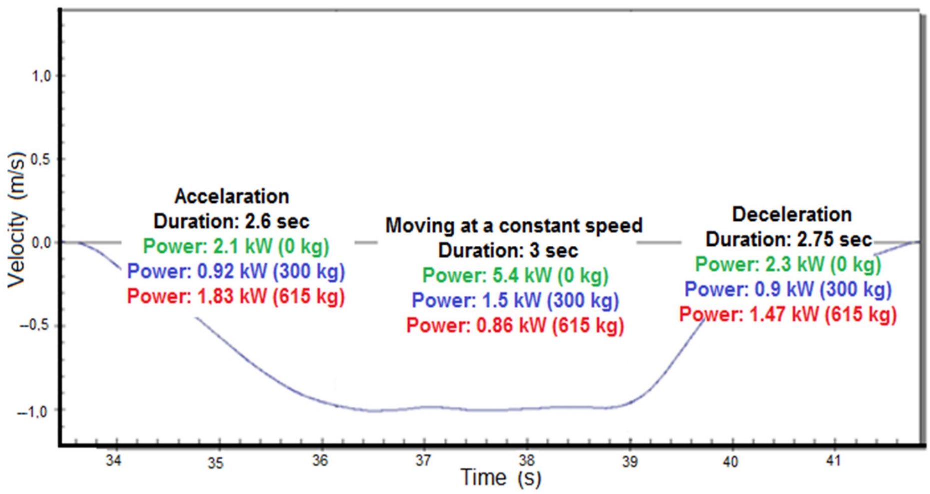


(**d**)

**Figure 5.** Typical programming curves of the elevator speed: (**a**) ascent movement with VVVF inverter; (**b**) descent movement with VVVF inverter; (**c**) ascent movement without VVVF inverter; (**d**) descent movement without VVVF inverter.

The user programs and introduces to the computer memory a desirable curve of the elevator's speed, as well as the first (acceleration) and second derivative of the speed (over acceleration). By introducing the curve shown in Figure 5a–d in the appropriate form, the optimization of the desired speed service and the comfort of the passengers during the journey is achieved [19]. The actual speed of the elevator is compared by the central computer using the encoder with the desired speed, which has been programmed in the computer memory. It controls the frequency of the motor supply so that it can adjust the actual speed to the desired value. Due to the fact that the comparison is almost continuous (70 tests per second), the actual curve is practically the same as the control target. As a result, there is a noticeable improvement in service speed achieved, especially during starting, stopping and balancing. Tables A25 and A26 calculate the time intervals of the lift movement based on the above movement curves.

The main advantages of using a VVVF inverter are the significant improvement in speed, which, in combination with the smooth movement of the elevator, especially during start, stop and balancing, creates an increased sense of comfort during transport. Moreover, the electrical motor draws less heat, which is limited to about half, thus enabling an unlimited number of allowable starts per hour, a longer electrical motor life and elimination of the need to install a cooling fan, which is usually noisy and energy-consuming. Finally, it achieves silent operation in combination with the fully equipped microcomputer and the elimination of surges due to strong harmonics, especially in low-frequency cases. In addition to the advantages at the electrical level, there are several positive aspects in the mechanical characteristics of the elevator. The mechanical construction is greatly simplified, since no reducer is needed for the variable transmission and no double-motor windings is required. By applying this control technique, significant advantages can be identified for the building itself. First of all, there are reduced requirements for sound and heat insulation of the machine room, the possibility of reducing the electric power supply line of the elevator due to the low starting current and elimination of the need to acquire equipment for the correction of the cosine in large-scale installations due to the high power factor.

In addition, the speed of the chamber is also determined using a digital speed sensor, which acts as a digital optical encoder used as a speed-pulse generator. Depending on the rate of generation of the pulses, the transducer can sense in real time the speed of movement of the chamber. Communication between the transducer and the motor is carried out using an encoder that is mounted on the motor shaft, providing appropriate speed and position information. The DC voltage at the output of the rectifier, the supply voltage and the motor current are used as inputs to the control unit, as well as calculations relating to the temperature of the variable-frequency drive and the temperature of the motor. This enables the microprocessor to calculate whether the variable-frequency unit is operating within the specified limit.

When the operation of the control unit is found from the parameters set, then the computer available in the inverter corrects the operations even in the case where the parameters are not restored and the drive system operates beyond the limits. In this case, the control unit operates automatically by interrupting the speed-control process. The system also has a display in order to monitor all the individual functions of both the motor and the lift, as well as the possibility of programming by adding or removing individual functions.

## 6. Energy Savings by Using a VVVF Technique

The mathematical model of an electrical motor, which is the significant element of the driving system, providing motion of the lift is described by the equations of the voltage and the evolving electromagnetic impetus, given as the follow:

$$\mathrm{V} = \mathrm{R}i + \frac{d}{dt}\,\mathrm{L}i \tag{4}$$

$$T_e = \frac{\left(\frac{P}{2}\right)}{2} i^T \frac{\partial L}{\partial \theta} i = \mathrm{J}\frac{dW_m}{dt} + \mathrm{b}W_m + T_f \quad (5)$$

where $W_m$ is the circular speed of the rotor (rad/s), $P$ is the number of poles, J is the constant of the inertia of the rotor and load (kg m$^2$), b is the motor friction constant due to losses (Nm/rad/s) and $T_f$ is the component of the load thrust not included in the constants J and b.

The developed electromagnetic impetus $T_e$ of a motor is the component of the currents absorbed by the motor at any given time to the angular velocity of the electrical motor:

$$T_e = \frac{P_e}{W_m} \quad (6)$$

The impetus balances the necessary mechanical thrust of the electrical motor and is given as the follow:

$$T_m = T_{Losses} + T_{Load} \quad (7)$$

The equation that determines the mechanical speed of the electrical motor is:

$$T_e - T_m = \mathrm{J}\frac{dW_m}{dt} \quad (8)$$

where for $T_e > T_m$ the motor accelerates, for $T_e = T_m$ the motor has a constant rotation speed and for $T_e < T_m$ the motor decelerates.

The power output of the motor depends on the lifting speed of the load and the active force. Thus, the following is applied:

$$\mathrm{N} = \frac{\mathrm{Fu}}{102\mathrm{n}} \quad (9)$$

where F is the active force (kg), u is the velocity of the cabin (m/s) and n is the efficiency of the system.

For the calculation of the active force and the counterweight, the following applies:

$$\mathrm{F} = \mathrm{B} + \mathrm{Q} - \mathrm{G} \quad (10)$$

$$\mathrm{G} = \mathrm{B} + \frac{1}{2}\mathrm{Q} \quad (11)$$

where B is the total weight of the cabin, suspension frame and cable (kg), Q is the passenger load (kg) and G is the weight of the counterweight (kg).

The speed of the chamber is given by:

$$\mathrm{u} = \frac{\pi D K \mathrm{n}}{60} \quad (12)$$

where $D$ is the diameter of the friction pulley (m), $K$ is ratio of the transferring reducer and n is the number of rotations of the motor (rpm).

The work produced for the vertical transfer of a particular load F in a distance S can be expressed as:

$$\mathrm{W} = \mathrm{FS} \quad (13)$$

The average power during a time dt is defined as the ratio of the work $dw$ and the equivalent time $dt$, as follows:

$$P_{av.} = \frac{dw}{dt} = \frac{1}{dt}\int_t^{t+dt} P(t)dt \quad (14)$$

The distance S can be derived from the motion diagram, shown in Figure 5a for the ascent movement and in Figure 5b for the descent movement, by the relation:

$$S = V_{max}[T - \frac{(t_1 + t_3)}{2}] \quad (15)$$

where $t_1$ = $V_{max}/C_1$ is the acceleration time, $t_3$ = $V_{max}/C_2$ is the deceleration time and $V_{max}$, $C_1$, $C_2$ are the maximum velocity of the constant-speed trajectory, acceleration and deceleration of the lift, respectively.

If in the last relation $t_1$ and $t_3$ are replaced by the above-mentioned relations involving $V_{max}$, $C_1$ and $C_3$, it follows that:

$$S = V_{max}T - \frac{1}{2}V_{max}{}^2(\frac{1}{C_1} + \frac{1}{C_3}) \quad (16)$$

In that respect, the total energy consumed by the elevator along the distance S between two stops with a constant load can be expressed by:

$$E = \frac{9.81F}{n}[V_{max}T - \frac{1}{2}V_{max}{}^2\left(\frac{1}{C_1} + \frac{1}{C_3}\right)] \quad (17)$$

Based on Equation (16), it may be concluded that the lower the acceleration and deceleration, the smoother the movement of the elevator and the higher the energy-saving rate achieved. At the same time, in order to achieve the maximum possible movement of the chamber, the average speed $V_m$ of the elevator is required to be satisfactory. Depending on the path the system is desired to follow, there is an appropriate adjustment of the speed–time curve u(t), which differs for each path and is given by the relation:

$$V_m = \frac{S}{\frac{S}{V_s} - t_0} \quad (18)$$

where $V_m$ is programmed trajectory velocity (m/s) and $t_0$ is the total time for boarding–disembarking and opening–closing of the doors (s).

## 7. Results

### *7.1. Current Consumption Electrical Motor PMSM and IM*

In order to access the operation and applicable power characteristics of an elevator using PMSM supplied by a VVVF inverter in conjunction with a vector control technique and an adapted smooth speed variation strategy based on the characteristics analyzed previously in Section 2, simulated and experimental results are compared to those obtained for an induction motor drive without a VVVF inverter. The characteristics of the two systems under consideration, including the characteristics of the lift, are reported in Tables 2 and 3, respectively.

**Table 2.** Characteristics of elevator and PMSM with VVVF inverter drive.

| Parameters | Symbol | Values |
|---|---|---|
| Rated Load | Q | 630 kg |
| Weight Chamber | P | 675 kg |
| Counterweight | CW | 990 kg |
| Rated Speed | U | 1 m/s |
| Route | R | 5.2 m |
| Electrical Motor | Gearless PMSM | 7.2 kW |
| Nominal Current | $I_{nom}$ | 12.24 A |
| DC Link Voltage | $V_{DC}$ | 380 V |
| Poles | P | 16 |
| Switching Frequency Inverter | $f_s$ | 5 kHz |
| Inertia | J | 0.0008 kg m$^2$ |

**Table 2.** *Cont.*

| Parameters | Symbol | Values |
|---|---|---|
| Inductance | $L_d$, $L_q$ | 0.00095 H |
| Stator Resistance | $R_s$ | 0.085 Ω |
| Nominal Torque | $T_n$ | 458.59 Nm |
| Flux Linkage | $\Psi_m$ | 0.192 Wb |
| Frequency | f | 20 Hz |
| Rated Speed | N | 150 rpm |

**Table 3.** Characteristics of elevator and induction motor without VVVF inverter drive.

| Parameters | Symbol | Values |
|---|---|---|
| Rated Load | Q | 630 kg |
| Weight Chamber | p | 630 kg |
| Counterweight | CW | 990 kg |
| Rated Speed | U | 1 m/s |
| Route | R | 6.1 m |
| Gear Ratio | $K$ | 1:9 |
| Electrical Motor | Geared IM | 7.3 kW |
| Nominal Current | $I_{nom}$ | 12.41 A |
| Stator Inductance | $L_s$ | 0.6780 H |
| Rotor Inductance | $L_r$ | 0.6780 H |
| Mutual Inductance | $L_m$ | 0.6722 H |
| Poles | P | 16 |
| Rotor Resistance | $R_r$ | 1.3950 Ω |
| Stator Resistance | $R_s$ | 1.4050 Ω |
| Inertia | J | 0.04 kg $m^2$ |
| Frequency | f | 50 Hz |
| Rated Voltage | V | 230/380 Volt |
| Rated Speed | N | 375 Rpm |

The experimental setup is shown in Figure 6. The energy analyzer was used for data extraction and processing, as shown in Figure 6a. In addition, in Figure 6b we observe the wiring of the VVVF inverter automation panel layout in order to measure the current and applicable power of the electrical motor in each lifting of a different chamber load.

The simulated stator current time variations during ascent and descent movements for an empty load, half-rated load and full load are shown in Figures 7–12. These figures illustrate that due to the counterweight action the currents are during half-load ascent and full-load descent operations. In the case of the empty chamber, the counterweight is heavier than the empty chamber, so in the descent the electrical motor has to lift the counterweight and thus has a higher load, more power and, therefore, higher consumption. Conversely, during the ascent of the empty chamber, the counterweight is lowered and with the help of gravity the electrical motor has a lower load, lower power and lower consumption. In the case of the half load the weight of the chamber is approximately the same as the weight of the counterweight, so in either the ascent or the descent the electrical motor has approximately the same load and the same consumption in both directions of motion. Moreover, in the case of the full load, the chamber has a higher weight than the counterweight and thus, in the ascent the electrical motor has a higher load and therefore more power and consumption is required, while in the descent of the full load due to gravity the electrical motor has a lower load, lower power and lower consumption. The main conclusion concerning the current consumption of the electrical motor based on variation in the chamber drive load is confirmed by the experimental data shown in Tables A1–A12 in Appendix A.

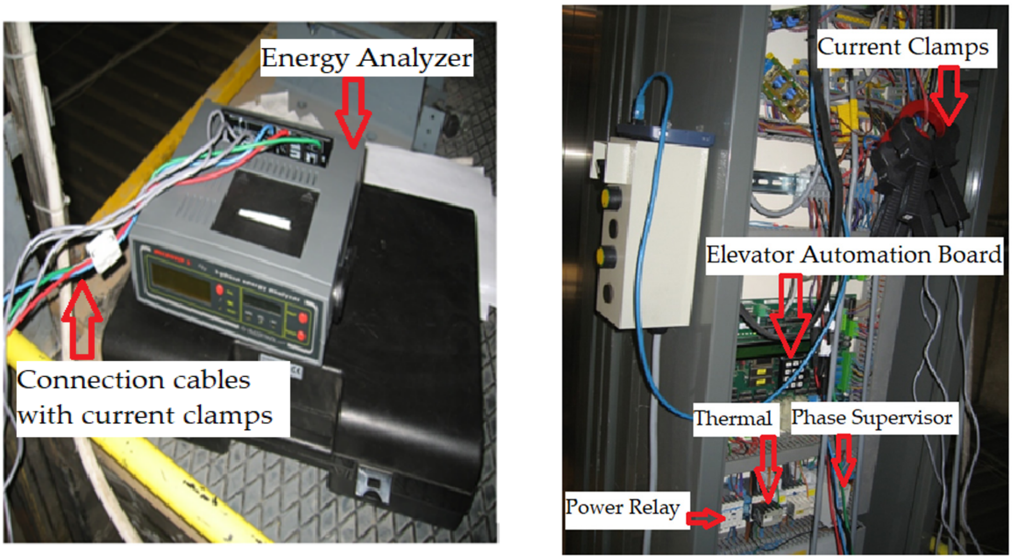


(**a**) (**b**)

**Figure 6.** Experimental setup: (**a**) energy Analyzer; (**b**) connection for measuring current and power consumption with the automation panel.

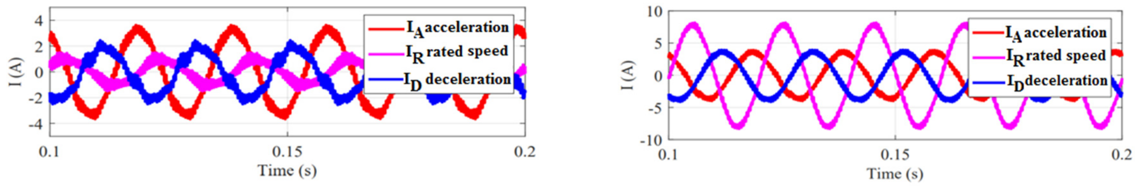


(**a**) (**b**)

**Figure 7.** Current time variation for PMSM drive with VVVF under empty load of 0 kg during: (**a**) ascent; (**b**) descent.

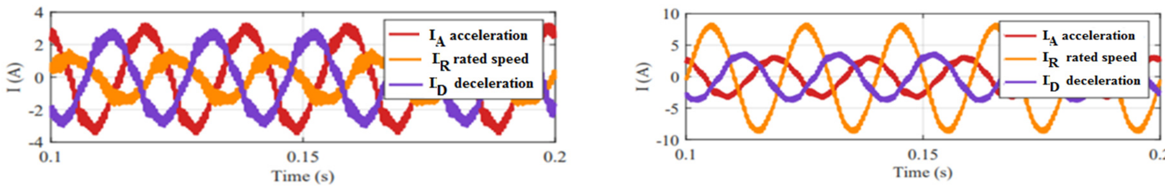


(**a**) (**b**)

**Figure 8.** Current time variation for the PMSM drive with VVVF under half-rated load of 300 kg during: (**a**) ascent; (**b**) descent.

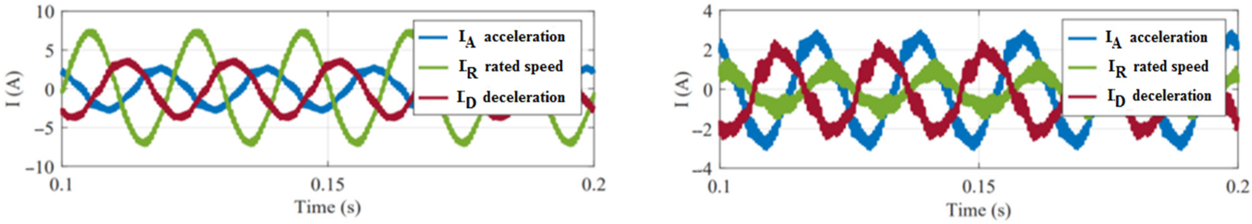


(**a**) (**b**)

**Figure 9.** Current time variation for the PMSM drive with VVVF under full-rated load of 615 kg during: (**a**) ascent; (**b**) descent.

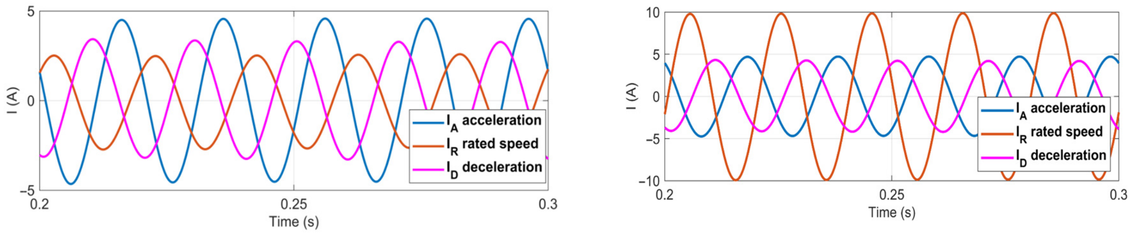


(**a**) (**b**)

**Figure 10.** Current time variation for the IM drive without VVVF under empty load of 0 kg during: (**a**) ascent; (**b**) descent.

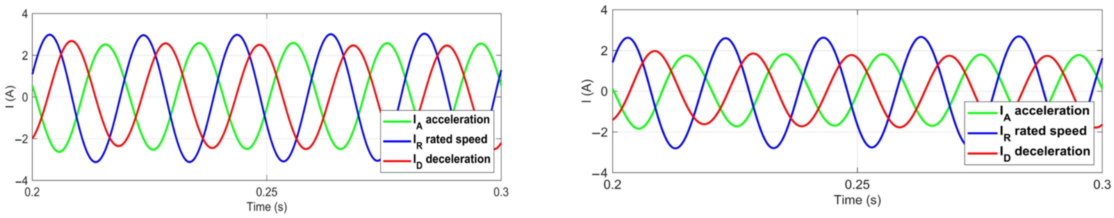


(**a**) (**b**)

**Figure 11.** Current time variation for IM drive without VVVF under half-rated load of 300 kg during: (**a**) ascent; (**b**) descent.

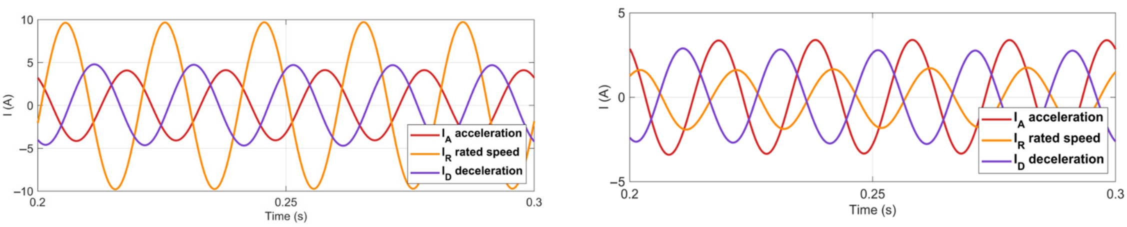


(**a**) (**b**)

**Figure 12.** Current time variation for IM drive without VVVF under full-rated load of 615 kg during: (**a**) ascent; (**b**) descent.

Using Tables A13–A24 in Appendix A, we can draw useful conclusions about the applicable power of the electrical motor. In the case with about half the rated load (300 kg) during the accent and descent of the chamber, we find that the power during acceleration and deceleration is the lowest possible. In addition, we have greater energy savings during acceleration and deceleration because there is an effect of the counterweight, the motor is operating under an empty load and its power only covers the mechanical friction losses. Similarly, in the case of a full load (615 kg) during the ascent of the chamber when the elevator is moving at constant speed, more power is observed, while during the descent we have almost zero power.

### 7.2. Pulses for PMSM with VVVF Inverter Driving

Figure 13 shows the pulse configuration of the inverter output supplying the electrical motor with appropriate voltage according to the modulation scheme. The inverter used for the experimental setup is a DC–AC converter with a constant DC voltage. In addition, both the amplitude of the voltage and its frequency are controlled. The power stage of the converter uses IGBT semiconductors due to the high power needed, the high input impedance, the low voltage drops and the high switching speed compared to other power semiconductors such as MOSFET [22]. Finally, a switching frequency of 5 kHz ensures the appropriate current waveform quality in stator windings.

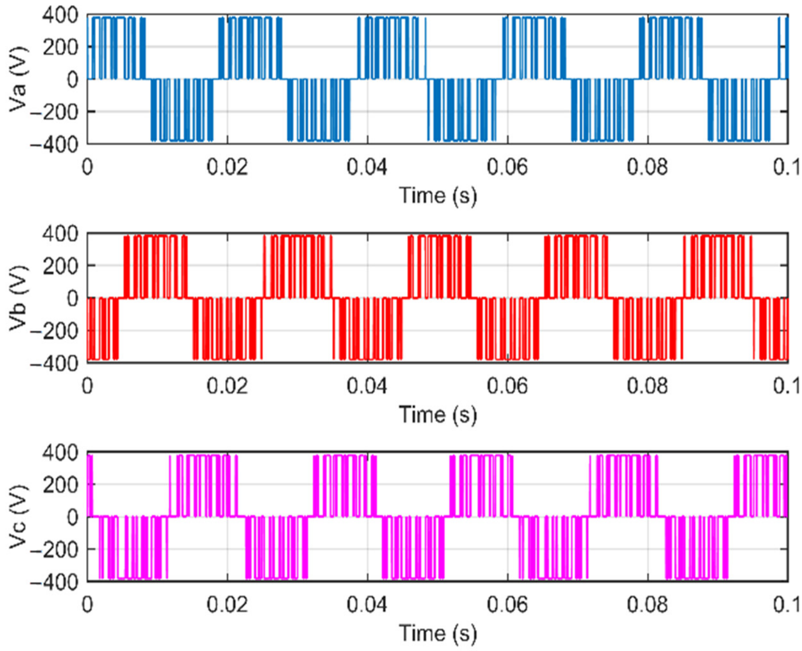


**Figure 13.** Sinusoidal pulse width modulation output of the inverter supplying the PMSM.

### *7.3. Speed of Electrical Motor for PMSM and IM*

The speed variation of the electrical motor also helps to draw useful conclusions concerning the operation of the chamber drive system. Figure 14a,b show the operating speeds of the induction motor supplied by the mains and of the PMSM driven by the inverter applying the VVVF technique. It can be observed that in the induction motor case important oscillation appears, illustrating a more pronounced transient effect. On the contrary, in the inverter-fed PMSM motor case, besides the energy savings, a smoother speed regulation is observed due to the proper tuning of the speed controllers available in the system. The appropriate speed setting of the electrical motor also determines the smooth chamber transition, as no particular accelerations and over-accelerations are observed during its operation.

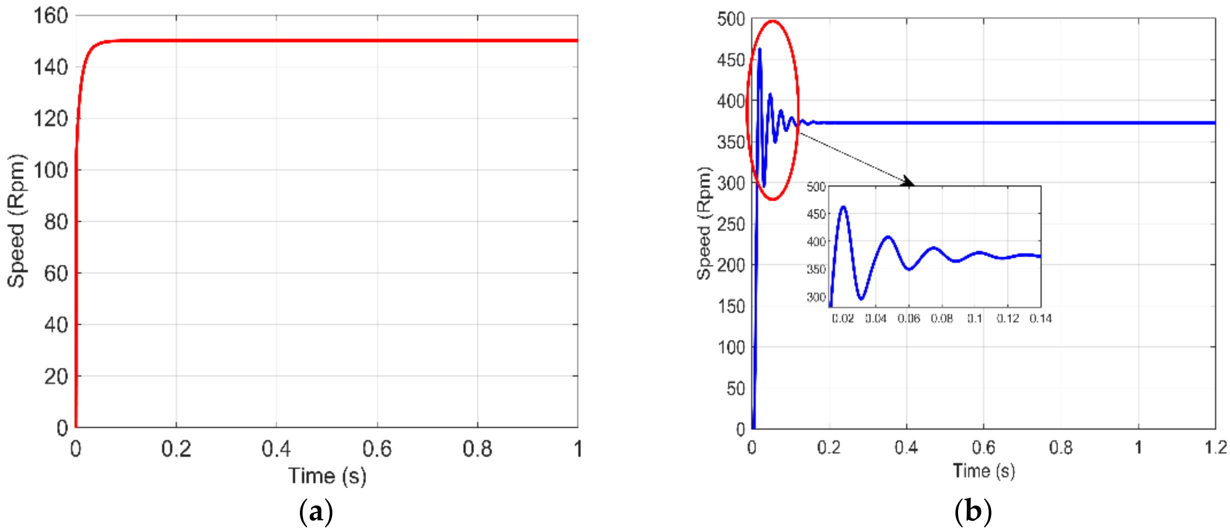


**Figure 14.** Rotor speed time variation of the electrical motor: (**a**) PMSM supplied by inverter applying VVVF technique; (**b**) induction motor supplied by the mains.

*7.4. Simulation Scenarios*

In the next step, typical scenarios of elevator loading have been considered, involving the floor calls as shown in Figure 15a,b. In the first case, a large number of calls with continuous lift movements was used, while in the second case, a smaller number of lift calls was chosen.

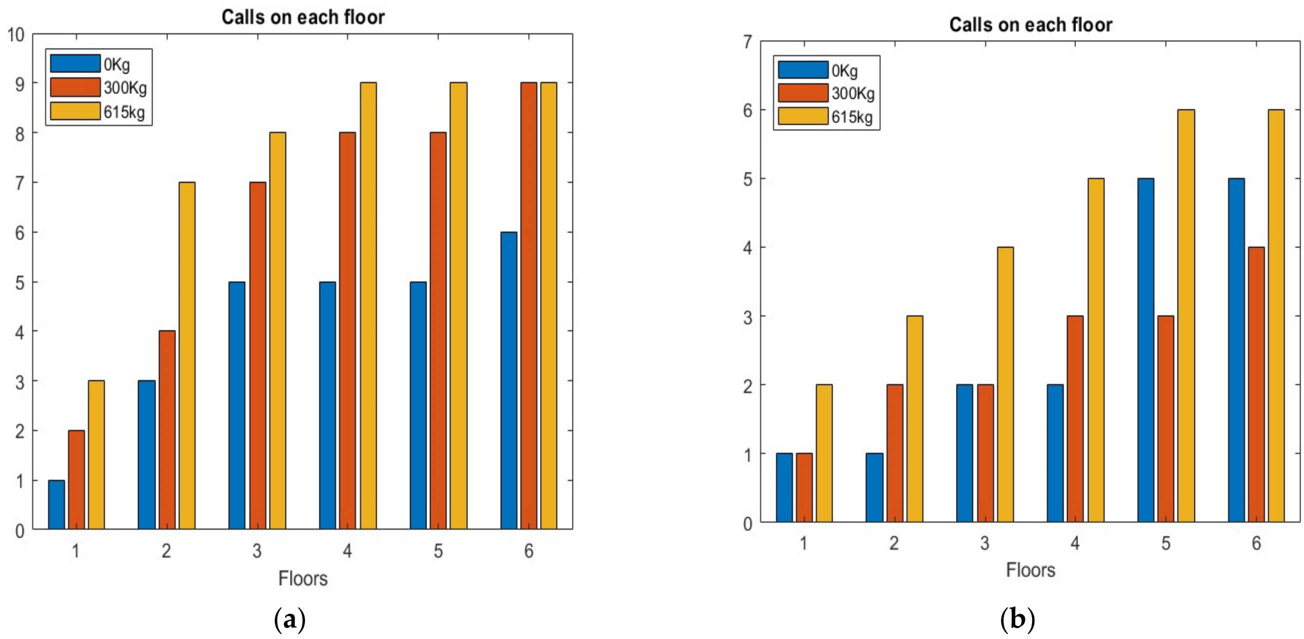


**Figure 15.** Measured scenarios of elevator calls in different floors: (**a**) with a higher number of calls; (**b**) with a smaller number of calls.

The simulation results are obtained by studying a typical lift movement in an urban block of flats and are obtained under assumptions. Moreover, it is worth emphasizing that in an office building or department store rather than the apartment building we studied, the elevator movement and possibly the chamber would have been differentiated. The elevator would have served a greater number of passengers and would possibly have been required to handle different loads to accommodate all users.

*7.5. Energy Consumption with VVVF and without VVVF*

Then, for each case we calculate the energy consumption during the ascent and descent of the elevator for the cases of drives with PMSM supplied by a VVVF inverter and an induction motor without a VVVF inverter, shown in Figure 16a,b and Figure 17a,b, respectively. The total number of floors for the building is six. Based on the elevator motion curves, using the height of each floor of 4.3 m and knowing that for the acceleration phase it is 0.5 m, for the constant-speed phase it is 3.3 m and for the deceleration phase it is 0.5 m, the energy consumption from the ground floor and from each floor is calculated as follows:

1. In the first part of the route and for a length of 0.5 m the elevator performs an accelerated movement and thus the energy consumed is the corresponding power depending on the load served by the lift (empty chamber, half load and full load) over the period of the accelerated movement of the lift.
2. During the second part of the route the elevator runs smoothly at a constant speed for the total length of the journey from the ground floor to the corresponding floor but reduced by 1 m, which is the part of the acceleration and deceleration of the chamber. Thus, the energy consumed in this section will have to be adjusted according to the time taken to complete the route. The time is adjusted according to the length of the route path that the elevator performs each time at a constant speed. Therefore, the energy consumed in this section will be the corresponding power depending on

the load it serves at any given time and the corresponding adjusted route time at constant speed.

3. Finally, in the last part of the route and for a length 0.5 m the elevator performs a deceleration movement and thus the energy consumed is the corresponding power according to the load served by the lift (empty chamber, half load and full load) over the period of the decelerated movement of the lift.

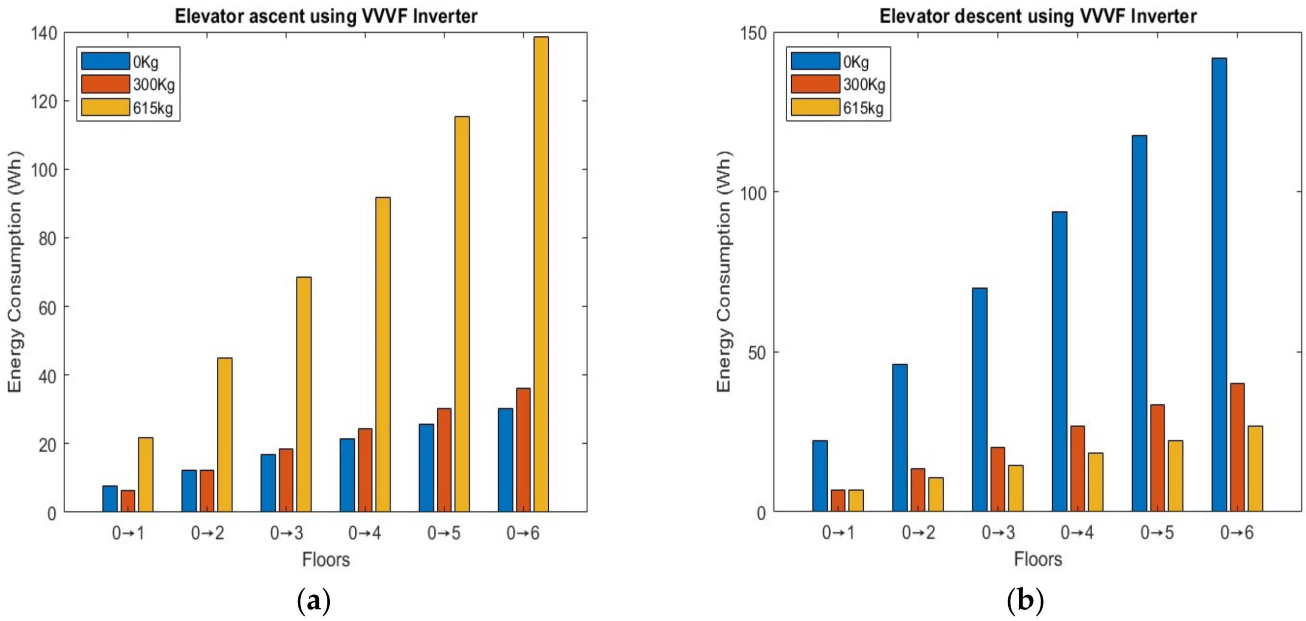


**Figure 16.** Energy consumption for PMSM drives with VVVF driving: (**a**) ascent; (**b**) descent.

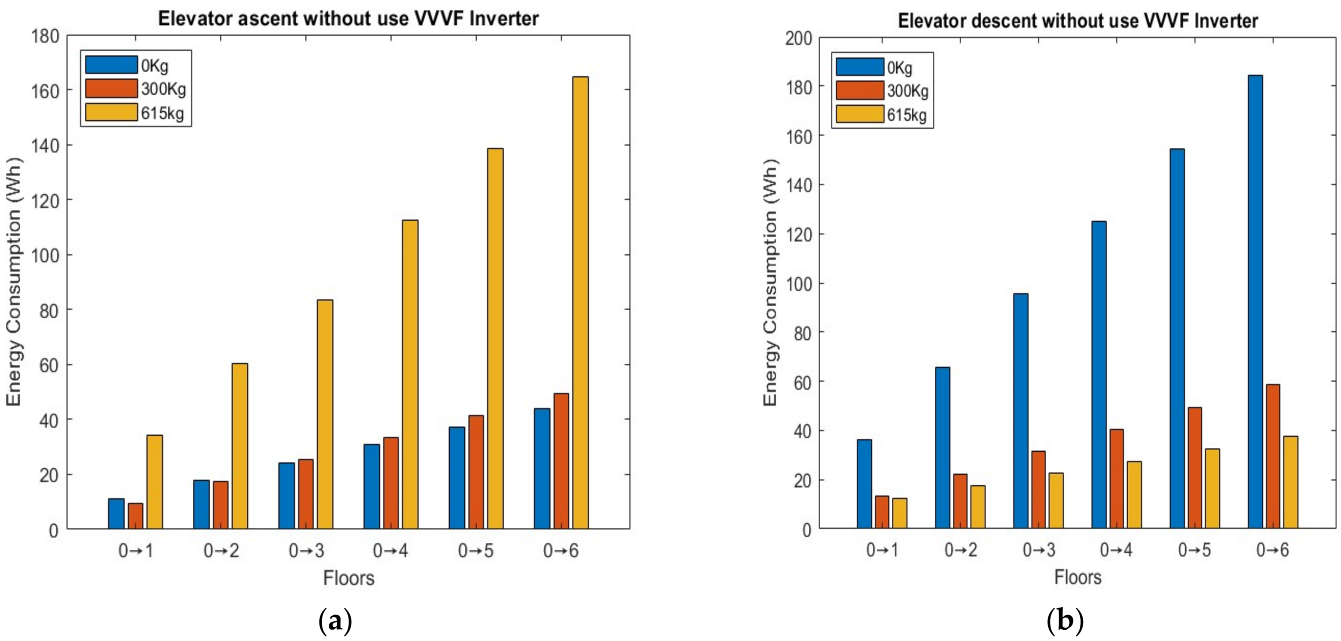


**Figure 17.** Energy consumption for drives IM without VVVF during: (**a**) ascent; (**b**) descent.

*7.6. Daily Energy Consumption with VVVF and without VVVF*

The respective measured daily energy consumption for the cases of drives with PMSM supplied by a VVVF inverter and an induction motor without a VVVF inverter are shown in Figure 18a,b and Figure 19a,b, respectively, which are in good agreement with the simulated results.

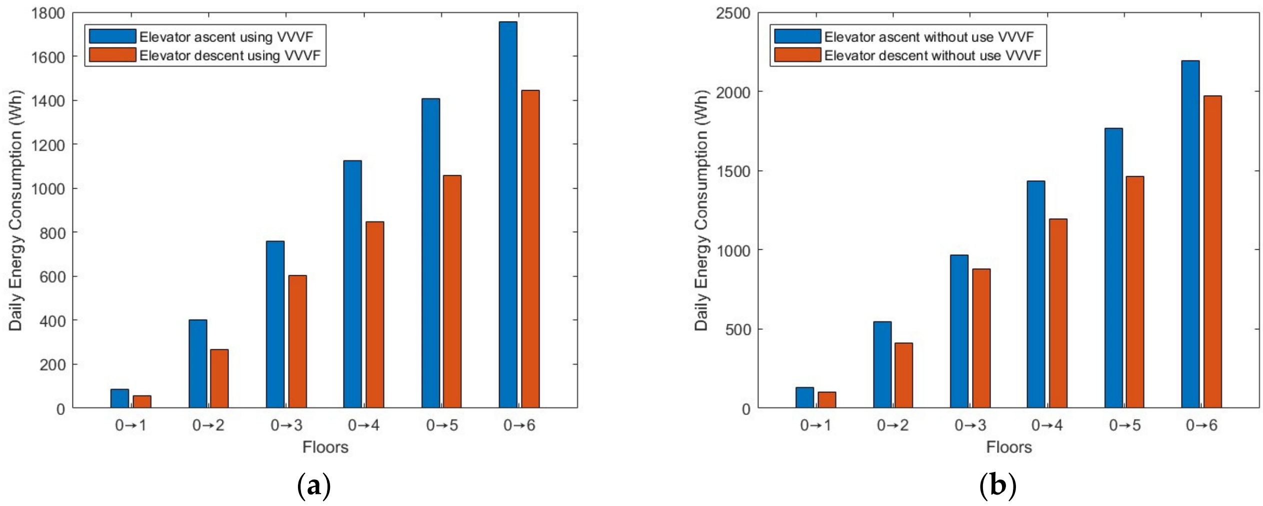


**Figure 18.** Daily energy consumption measured in case 1 for: (**a**) PMSM drive with VVVF; (**b**) IM drive without VVVF.

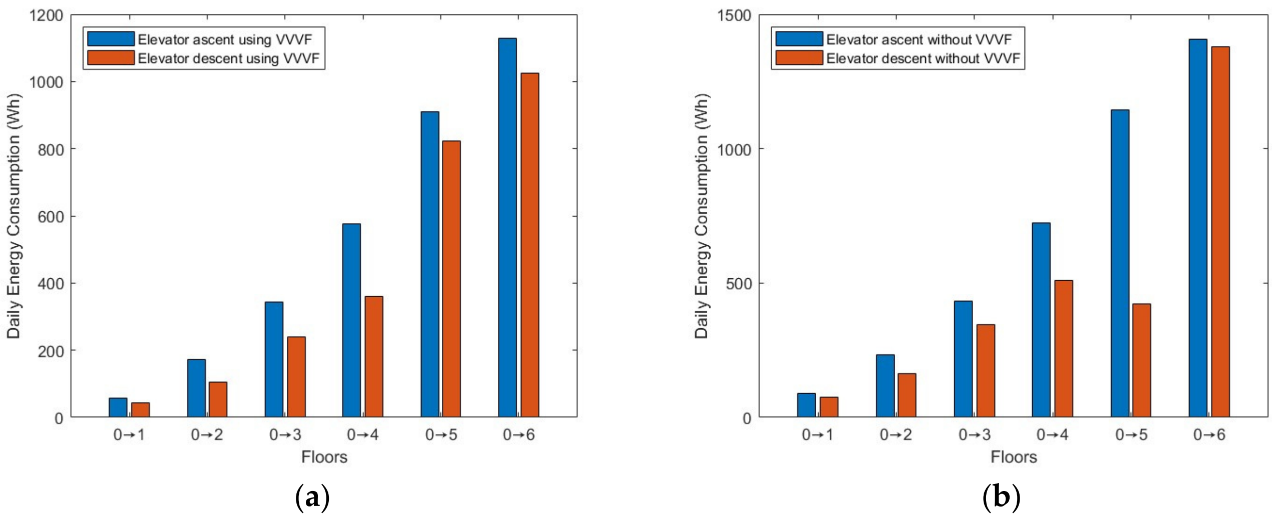


**Figure 19.** Daily energy consumption measured in case 2 for: (**a**) PMSM drive with VVVF; (**b**) IM drive without VVVF.

### *7.7. Total Energy Efficiency*

According to the calculation of daily energy consumption, an energy savings rate of 24.76% is achieved for the first call number scenario and 16.35% for the second scenario shown in Figure 20a and Figure 20b, respectively. It may be noted that such important energy savings are achieved in cases of approximately half-rated loading, while in cases involving frequent full-load operation the energy savings assessed are relatively lower.

In the case 1 the total energy savings is:

$$\text{Energy Savings }(\%) = \frac{13048.16 - 9817.15}{13048.16} \times 100\% = 24.76\% \quad (19)$$

In the case 2 the total energy savings is:

$$\text{Energy Savings }(\%) = \frac{6420.59 - 5370.25}{6420.59} \times 100\% = 16.35\% \quad (20)$$

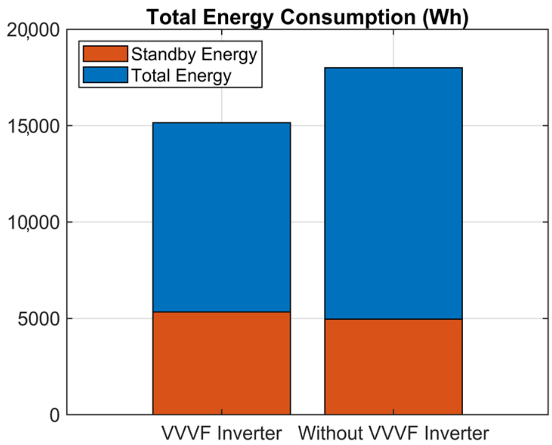


(a)

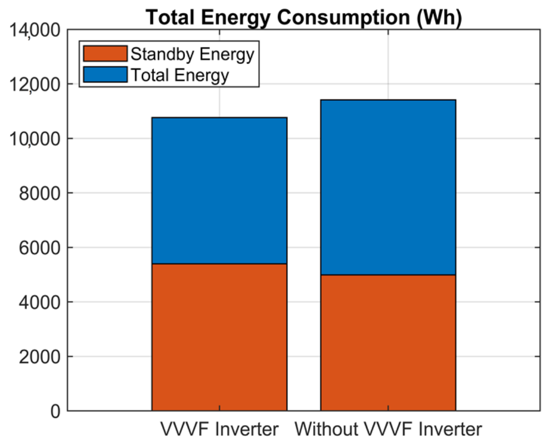


(b)

**Figure 20.** Total measured energy consumption: (**a**) scenario 1; (**b**) scenario 2.

### *7.8. VDI 4707*

This method is a research process on the energy efficiency of elevators according to some specific criteria regarding the amount of energy they consume, but also helping to draw useful conclusions regarding the efficiency of the building studied. Their ranking is related to the energy consumed during standby and during lifting. The energy standby is determined 10 min after the last lift is completed, while the lifting energy refers to the consumption during the motion for a given route, always taking into account the corresponding energy spent on opening the doors [23].

Based on the experimental data, the standby consumption for an elevator with VVVF is 232 W while that without VVVF is 215 W. The elevator is in motion daily for about one hour for the first case and about thirty-five minutes for the second case with VVVF driving. In contrast, the lift without VVVF driving is in operation for fifty-four minutes in the first case and thirty-eight minutes in the second case. Therefore, as Figure 20 shows, we observe that the energy consumption increases significantly, as the elevator also consumes energy during the standby time. The total travel distance of the lift is 3749.6 m for the first case and 2046 m for the second case. The total travel times of the lift both with VVVF driving and without the use of a VVVF inverter are calculated in Tables A25 and A26, respectively.

Tables A27 and A29–A32 show the use category and energy efficiency class of the two elevators. In the first case, with a large number of calls, the lifts belong to usage category 2 and the energy-efficiency class with the VVVF driving inverter is E and without the VVVF inverter is F. In the second case, with the lowest number of calls, the lifts belong to usage category 1 and the energy-efficiency class with the VVVF driving inverter is E and without the VVVF inverter is E.

In case 1 the total energy savings including the standby energy consumption of the elevator is:

$$\text{Energy Savings } (\%) = \frac{18006.06 - 15153.15}{18006.06} \times 100\% = 15.84\% \tag{21}$$

In the case 2 the total energy savings including the standby energy consumption of the elevator is:

$$\text{Energy Savings } (\%) = \frac{11412.89 - 10764.25}{11412.89} \times 100\% = 5.68\% \tag{22}$$

## 8. Discussion

In addition, there are alternative methods that can lead to a higher percentage energy savings.

- Similarly, returning some of the energy back to the grid using an inverter with a regenerative mechanism would result in energy savings rates of over 50% in Figure 21a,b [24]. Using braking, the electrical motor acts as a generator by converting mechanical energy into electrical energy, which is dissipated as heat through thermal resistance. Through a regenerative mode, this energy is collected and fed into a building or the city's electricity grid [25]. This arrangement would require to the use of a transformer and more sophisticated power electronics. Thus, in this way energy recovery during braking, replacements of the braking resistors, reduced maintenance of the drive system and additional reduction in heat emissions are achieved. The regenerative mechanism can be applied when the developing motor torque is in the opposite direction to the load torque. This can happen is two cases, either when the load is descending by gravity or in the case of the load rising by parallel braking (the load is rising upwards but the motor is trying to brake (accelerate)) [26]. The brakes are applied so that the electrical motor can maintain its nominal speed. Based on Table A28 and using the motion curves of the elevator in Figure 5, we calculate for each different load the total travel interval of the chamber and the efficiency of the drive system in general to see the potential for additional energy savings using regenerative braking. In the case of ascent with 0 kg load during the constant-speed movement of the lift and in the case of descent with 300 kg with VVVF inverter driving we observe a very low-efficiency system. Moreover, in the cases of ascent and descent with a 300 kg load without a driving VVVF inverter we observe the same effect because the electrical motor works as a generator; therefore, it is possible by using an appropriate regenerative mechanism to save additional energy for the system.
- The elevator consumes energy even when it is stopped and is in standby mode. This consumption is due to the use of the power electronics, the indicator lights that show the status of the lift, the PLC and the sensors of the lift. In order to avoid this particular case, which results in additional energy consumption, the DC power supply can be accomplished using a low-power photovoltaic installation for battery charging, as shown in Figure 22. In this way, a 4–5% additional energy savings in achieved over using VVVF technology. The main advantages are that 80% less energy is required depending on the uses performed by the lift; it is powered by one small system, two photovoltaic panels and two batteries; it can be an integrated building evacuation system (BEMS) in which people cannot be trapped in it, as it is continuously powered by the batteries; and there is the possibility of providing additional 230 VAC electricity. Moreover, it has a longer lifespan, as the power generation is of better quality and gives the possibility of 30 movements per day, providing autonomy for 30 days [27–31].
- This paper illustrated through experimental validation that, by implementing a particular loading pattern in the control of the elevator, energy savings of up to almost 25% can be achieved, corresponding to the highest level attainable in such applications [32], and can be of reference value, offering great services for operators in the field.

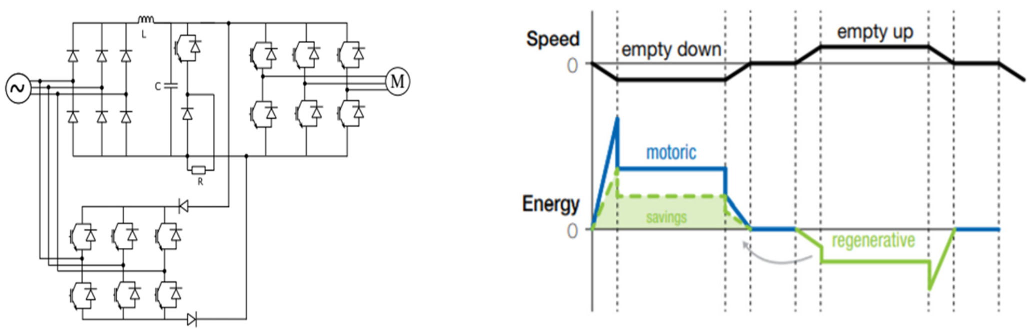


(**a**) (**b**)

**Figure 21.** Regenerative mechanism: (**a**) basic structure of components of a regenerative mechanism; (**b**) energy savings.

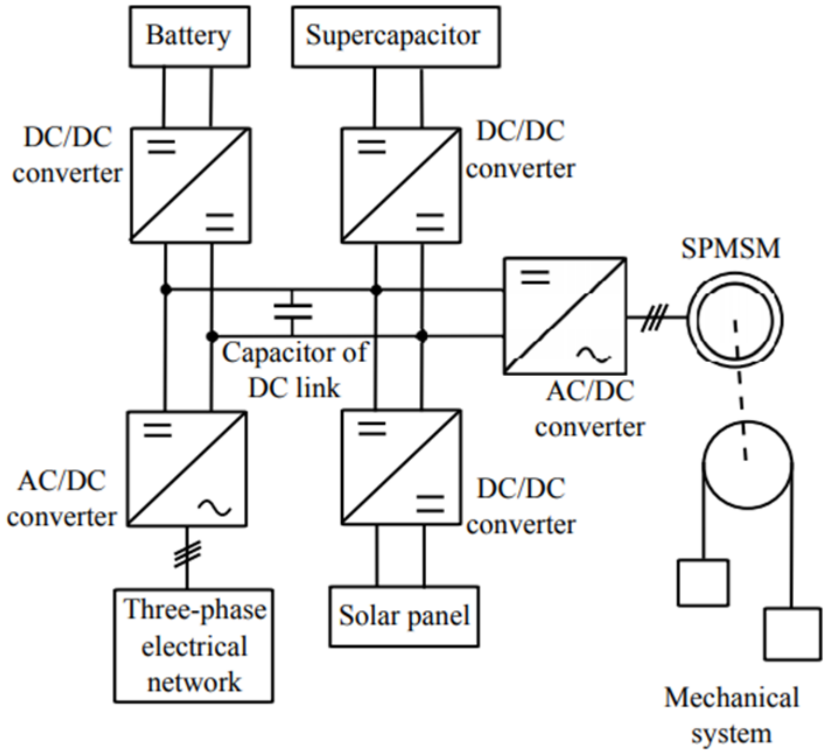


**Figure 22.** Solar lift operating mechanism [32].

## 9. Conclusions

Based on the simulations and experimental validations presented, concerning many elevator load cases, it is concluded that important energy savings can be achieved through the VVVF inverter application examined. It may be noted, however, that the energy savings percentage obtained depends importantly on the lift loading conditions, the active force as well as the number of calls/starts considered. Moreover, no significant deviation in the movement of the chamber has been observed under empty-chamber conditions. Particular attention should be paid to the calculation of the counterweight at half the rated load, as, if not calculated currently they can lead to higher energy consumption rates and create problems in the total energy savings percentage. In the case of a full load, the VVVF system adopted offered a lower percentage of energy savings, while a higher percentage of energy savings has been assessed under operating conditions involving half the rated power. The active lift force that occurs at any given time is responsible for consuming a large part of the specific energy. Regarding the choice of counterweight, a lower weight value results in smaller energy consumption under empty-chamber conditions, but in higher consumption at full chamber loading. Finally, in the case with a lower number of calls, the standby load is higher, so that significant energy savings are not achieved with the use of the inverter. Similarly, in the case where the lift receives few calls during the day, the desired savings are not achieved and therefore, the energy class is not changed.

**Author Contributions:** Conceptualization, V.I.V. and A.G.K.; methodology, V.I.V., T.S.K. and A.G.K.; software, V.I.V.; validation, V.I.V., T.S.K. and A.G.K.; formal analysis, V.I.V. and A.G.K.; investigation, V.I.V.; data curation, V.I.V., T.S.K. and A.G.K.; writing—original draft preparation, V.I.V.; writing—review and editing, A.G.K.; visualization, V.I.V. and A.G.K.; supervision, A.G.K. All authors have read and agreed to the published version of the manuscript.

**Funding:** This research received no external funding.

**Data Availability Statement:** Not applicable.

**Conflicts of Interest:** The authors declare no conflict of interest.

## Appendix A

**Table A1.** Current consumption with VVVF inverter driving for 0 kg during the ascent.

| Acceleration Current (A) | Constant-Speed Current (A) | Deceleration Current (A) |
|---|---|---|
| 2.91 | 1.54 | 2.48 |
| 2.97 | 1.39 | 2.35 |
| 2.94 | 1.49 | 2.36 |
| 3.05 | 1.51 | 2.38 |
| 2.9 | 1.44 | 2.33 |
| 2.99 | 1.55 | 2.49 |
| 2.99 | 1.51 | 2.38 |
| 2.93 | 1.5 | 2.36 |
| 2.91 | 1.52 | 2.39 |
| 2.88 | 1.54 | 2.34 |

**Table A2.** Current consumption with VVVF inverter driving for 0 kg during the descent.

| Acceleration Current (A) | Constant-Speed Current (A) | Deceleration Current (A) |
|---|---|---|
| 3.29 | 7.97 | 3.64 |
| 3.08 | 8.18 | 3.66 |
| 3.01 | 8.04 | 3.63 |
| 3.04 | 8.02 | 3.52 |
| 3.11 | 7.97 | 3.44 |
| 2.98 | 7.88 | 3.43 |
| 3.05 | 7.93 | 3.67 |
| 3.03 | 8.10 | 3.44 |
| 3.12 | 7.98 | 3.42 |
| 2.99 | 8.04 | 3.41 |

**Table A3.** Current consumption with VVVF inverter driving for 300 kg during the ascent.

| Acceleration Current (A) | Constant-Speed Current (A) | Deceleration Current (A) |
|---|---|---|
| 1.40 | 1.82 | 1.49 |
| 1.36 | 1.80 | 1.45 |
| 1.38 | 1.80 | 1.47 |
| 1.44 | 1.88 | 1.49 |
| 1.55 | 1.89 | 1.48 |
| 1.41 | 1.82 | 1.44 |
| 1.50 | 1.86 | 1.46 |
| 1.36 | 1.83 | 1.50 |
| 1.48 | 1.81 | 1.43 |
| 1.49 | 1.90 | 1.44 |

**Table A4.** Current consumption with VVVF inverter driving for 300 kg during the descent.

| Acceleration Current (A) | Constant-Speed Current (A) | Deceleration Current (A) |
|---|---|---|
| 1.53 | 2.36 | 1.53 |
| 1.37 | 2.35 | 1.48 |
| 1.37 | 2.26 | 1.54 |
| 1.51 | 2.24 | 1.42 |
| 1.40 | 2.32 | 1.58 |
| 1.51 | 2.62 | 1.48 |
| 1.48 | 2.25 | 1.46 |
| 1.84 | 2.12 | 1.51 |
| 1.50 | 2.31 | 1.48 |
| 1.37 | 2.23 | 1.45 |

**Table A5.** Current consumption with VVVF inverter driving for 615 kg during the ascent.

| Acceleration Current (A) | Constant-Speed Current (A) | Deceleration Current (A) |
|---|---|---|
| 2.88 | 7.47 | 3.64 |
| 3.00 | 7.32 | 3.61 |
| 2.91 | 7.34 | 3.61 |
| 2.90 | 7.34 | 3.63 |
| 2.86 | 7.47 | 3.53 |
| 2.84 | 7.57 | 3.57 |
| 2.80 | 7.52 | 3.71 |
| 2.85 | 7.36 | 3.55 |
| 2.91 | 7.55 | 3.34 |
| 2.86 | 7.49 | 3.61 |

**Table A6.** Current consumption with VVVF inverter driving for 615 kg during the descent.

| Acceleration Current (A) | Constant-Speed Current (A) | Deceleration Current (A) |
|---|---|---|
| 2.69 | 1.47 | 2.28 |
| 2.64 | 1.45 | 2.32 |
| 2.66 | 1.46 | 2.23 |
| 2.71 | 1.44 | 2.33 |
| 2.66 | 1.43 | 2.41 |
| 2.69 | 1.43 | 2.29 |
| 2.66 | 1.43 | 2.18 |
| 2.71 | 1.42 | 2.35 |
| 2.71 | 1.44 | 2.46 |
| 2.66 | 1.41 | 2.40 |

**Table A7.** Current consumption without VVVF inverter driving for 0 kg during the ascent.

| Acceleration Current (A) | Constant-Speed Current (A) | Deceleration Current (A) |
|---|---|---|
| 4.21 | 2.27 | 3.62 |
| 4.28 | 2.23 | 3.58 |
| 4.14 | 2.29 | 3.76 |
| 4.32 | 2.34 | 3.55 |
| 4.35 | 2.37 | 3.68 |
| 4.30 | 2.30 | 3.72 |
| 4.12 | 2.33 | 3.65 |
| 4.44 | 2.35 | 3.61 |
| 4.48 | 2.22 | 3.59 |
| 4.37 | 2.38 | 3.75 |

**Table A8.** Current consumption without VVVF inverter driving for 0 kg during the descent.

| Acceleration Current (A) | Constant-Speed Current (A) | Deceleration Current (A) |
|---|---|---|
| 4.49 | 9.82 | 4.12 |
| 4.58 | 9.77 | 4.18 |
| 4.63 | 9.80 | 4.06 |
| 4.44 | 9.86 | 4.04 |
| 4.43 | 9.83 | 4.10 |
| 4.47 | 9.82 | 4.14 |
| 4.52 | 9.74 | 4.06 |
| 4.54 | 9.75 | 4.09 |
| 4.46 | 9.90 | 4.14 |
| 4.53 | 9.77 | 4.11 |

**Table A9.** Current consumption without VVVF inverter driving for 300 kg during the ascent.

| Acceleration Current (A) | Constant-Speed Current (A) | Deceleration Current (A) |
|---|---|---|
| 2.28 | 2.87 | 2.19 |
| 2.32 | 2.79 | 2.22 |
| 2.39 | 2.97 | 2.28 |
| 2.19 | 2.91 | 2.14 |
| 2.22 | 2.84 | 2.25 |
| 2.27 | 3.05 | 2.12 |
| 2.27 | 2.75 | 2.21 |
| 2.29 | 3.04 | 2.15 |
| 2.31 | 2.86 | 2.21 |
| 2.32 | 2.97 | 2.17 |

**Table A10.** Current consumption without VVVF inverter driving for 300 kg during the descent.

| Acceleration Current (A) | Constant-Speed Current (A) | Deceleration Current (A) |
|---|---|---|
| 1.72 | 2.62 | 1.59 |
| 1.74 | 2.69 | 1.62 |
| 1.68 | 2.55 | 1.66 |
| 1.69 | 2.61 | 1.74 |
| 1.77 | 2.58 | 1.75 |
| 1.62 | 2.52 | 1.68 |
| 1.65 | 2.54 | 1.78 |
| 1.70 | 2.51 | 1.72 |
| 1.65 | 2.66 | 1.69 |
| 1.66 | 2.74 | 1.80 |

**Table A11.** Current consumption without VVVF inverter driving for 615 kg during the ascent.

| Acceleration Current (A) | Constant-Speed Current (A) | Deceleration Current (A) |
|---|---|---|
| 4.00 | 9.64 | 4.95 |
| 4.08 | 9.48 | 4.97 |
| 4.12 | 9.52 | 4.91 |
| 4.12 | 9.52 | 4.91 |
| 4.04 | 9.51 | 5.02 |
| 3.84 | 9.44 | 4.85 |
| 3.93 | 9.62 | 4.93 |
| 3.91 | 9.48 | 4.87 |
| 4.09 | 9.50 | 4.93 |
| 4.12 | 9.52 | 9.00 |

**Table A12.** Current consumption without VVVF inverter driving for 615 kg during the descent.

| Acceleration Current (A) | Constant-Speed Current (A) | Deceleration Current (A) |
|---|---|---|
| 3.23 | 1.58 | 2.54 |
| 3.30 | 1.55 | 2.55 |
| 3.41 | 1.62 | 2.50 |
| 3.32 | 1.65 | 2.52 |
| 3.37 | 1.60 | 2.44 |
| 3.25 | 1.59 | 2.47 |
| 3.28 | 1.55 | 2.51 |
| 3.29 | 1.58 | 2.56 |
| 3.34 | 1.64 | 2.45 |
| 3.29 | 1.66 | 2.48 |

**Table A13.** Applicable power with VVVF inverter driving for 0 kg during the ascent.

| Acceleration Power (kW) | Constant-Speed Power (kW) | Deceleration Power (kW) |
|---|---|---|
| 2.00 | 0.950 | 1.52 |
| 1.99 | 0.929 | 1.53 |
| 2.00 | 0.909 | 1.54 |
| 2.01 | 0.931 | 1.54 |
| 2.08 | 0.946 | 1.55 |
| 1.99 | 0.938 | 1.58 |
| 2.01 | 0.917 | 1.56 |
| 1.99 | 0.936 | 1.47 |
| 1.98 | 0.929 | 1.44 |
| 2.00 | 0.931 | 1.51 |

**Table A14.** Applicable power with VVVF inverter driving for 0 kg during the descent.

| Acceleration Power (kW) | Constant-Speed Power (kW) | Deceleration Power (kW) |
|---|---|---|
| 2.30 | 5.70 | 2.00 |
| 2.11 | 5.29 | 2.45 |
| 2.03 | 5.31 | 2.26 |
| 2.05 | 5.35 | 2.44 |
| 2.04 | 5.3 | 2.38 |
| 2.11 | 5.37 | 2.41 |
| 2.06 | 5.32 | 2.32 |
| 2.07 | 5.52 | 2.17 |
| 2.11 | 5.47 | 2.21 |
| 2.12 | 5.38 | 2.11 |

**Table A15.** Applicable power with VVVF inverter driving for 300 kg during the ascent.

| Acceleration Power (kW) | Constant-Speed Power (kW) | Deceleration Power (kW) |
|---|---|---|
| 0.941 | 1.28 | 0.931 |
| 0.970 | 1.24 | 0.899 |
| 0.918 | 1.22 | 0.924 |
| 0.927 | 1.26 | 0.894 |
| 0.909 | 1.21 | 0.900 |
| 0.915 | 1.18 | 0.870 |
| 0.953 | 1.25 | 0.910 |
| 0.918 | 1.20 | 0.889 |
| 0.930 | 1.19 | 0.898 |
| 0.900 | 1.22 | 0.907 |

**Table A16.** Applicable power with VVVF inverter driving for 300 kg during the descent.

| Acceleration Power (kW) | Constant-Speed Power (kW) | Deceleration Power (kW) |
|---|---|---|
| 0.948 | 1.53 | 0.914 |
| 0.924 | 1.56 | 0.894 |
| 0.930 | 1.51 | 0.89 |
| 0.923 | 1.55 | 0.889 |
| 0.922 | 1.46 | 0.918 |
| 0.915 | 1.54 | 0.873 |
| 0.926 | 1.48 | 0.936 |
| 0.940 | 1.51 | 0.899 |
| 0.941 | 1.53 | 0.897 |
| 0.920 | 1.47 | 0.894 |

**Table A17.** Applicable power with VVVF inverter driving for 615 kg during the ascent.

| Acceleration Power (kW) | Constant-Speed Power (kW) | Deceleration Power (kW) |
|---|---|---|
| 1.97 | 4.90 | 2.43 |
| 1.95 | 4.84 | 2.38 |
| 1.95 | 4.77 | 2.42 |
| 1.98 | 4.81 | 2.42 |
| 1.97 | 4.88 | 2.46 |
| 1.97 | 4.96 | 2.46 |
| 1.92 | 4.85 | 2.43 |
| 1.97 | 4.92 | 2.47 |
| 2.02 | 4.91 | 2.44 |
| 1.98 | 5.03 | 2.44 |

**Table A18.** Applicable power with VVVF inverter driving for 615 kg during the descent.

| Acceleration Power (kW) | Constant-Speed Power (kW) | Deceleration Power (kW) |
|---|---|---|
| 1.84 | 0.878 | 1.46 |
| 1.87 | 0.878 | 1.46 |
| 1.83 | 0.867 | 1.47 |
| 1.83 | 0.858 | 1.48 |
| 1.80 | 0.856 | 1.47 |
| 1.82 | 0.857 | 1.48 |
| 1.83 | 0.861 | 1.49 |
| 1.85 | 0.865 | 1.48 |
| 1.84 | 0.856 | 1.47 |
| 1.83 | 0.858 | 1.46 |

**Table A19.** Applicable power without VVVF inverter driving for 0 kg during the ascent.

| Acceleration Power (kW) | Constant-Speed Power (kW) | Deceleration Power (kW) |
|---|---|---|
| 2.39 | 1.31 | 2.00 |
| 2.35 | 1.32 | 2.20 |
| 2.42 | 1.36 | 2.15 |
| 2.38 | 1.29 | 2.06 |
| 2.46 | 1.33 | 1.94 |
| 2.32 | 1.30 | 1.99 |
| 2.48 | 1.28 | 2.06 |
| 2.45 | 1.25 | 1.92 |
| 2.36 | 1.29 | 1.96 |
| 2.40 | 1.26 | 1.98 |

**Table A20.** Applicable power without VVVF inverter driving for 0 kg during the descent.

| Acceleration Power (kW) | Constant-Speed Power (kW) | Deceleration Power (kW) |
|---|---|---|
| 2.38 | 6.02 | 2.68 |
| 2.45 | 5.94 | 2.75 |
| 2.40 | 5.90 | 2.70 |
| 2.38 | 5.87 | 2.66 |
| 2.47 | 5.79 | 2.52 |
| 2.30 | 5.92 | 2.70 |
| 2.48 | 5.91 | 2.49 |
| 2.40 | 5.87 | 2.55 |
| 2.37 | 5.84 | 2.52 |
| 2.42 | 5.97 | 2.47 |

**Table A21.** Applicable power without VVVF inverter for 300 kg during the ascent.

| Acceleration Power (kW) | Constant-Speed Power (kW) | Deceleration Power (kW) |
|---|---|---|
| 1.25 | 1.50 | 1.22 |
| 1.31 | 1.68 | 1.24 |
| 1.31 | 1.65 | 1.28 |
| 1.26 | 1.62 | 1.16 |
| 1.22 | 1.71 | 1.18 |
| 1.34 | 1.63 | 1.19 |
| 1.18 | 1.52 | 1.23 |
| 1.19 | 1.58 | 1.12 |
| 1.22 | 1.57 | 1.16 |
| 1.22 | 1.60 | 1.26 |

**Table A22.** Applicable power without VVVF inverter for 300 kg during the descent.

| Acceleration Power (kW) | Constant-Speed Power (kW) | Deceleration Power (kW) |
|---|---|---|
| 1.12 | 1.85 | 1.12 |
| 1.09 | 1.81 | 1.11 |
| 1.16 | 1.87 | 1.15 |
| 1.18 | 1.80 | 1.07 |
| 1.20 | 1.85 | 1.09 |
| 1.16 | 1.73 | 1.10 |
| 1.14 | 1.78 | 1.12 |
| 1.15 | 1.75 | 1.14 |
| 1.17 | 1.86 | 1.07 |
| 1.17 | 1.78 | 1.08 |

**Table A23.** Applicable power without VVVF inverter for 615 kg during the ascent.

| Acceleration Power (kW) | Constant-Speed Power (kW) | Deceleration Power (kW) |
|---|---|---|
| 2.33 | 5.29 | 2.72 |
| 2.24 | 5.25 | 2.78 |
| 2.26 | 5.12 | 2.74 |
| 2.12 | 5.24 | 2.86 |
| 2.20 | 5.19 | 2.81 |
| 2.32 | 5.32 | 2.71 |
| 2.19 | 5.19 | 2.58 |
| 2.06 | 5.08 | 2.64 |
| 2.11 | 5.18 | 2.62 |
| 2.16 | 5.21 | 2.59 |

**Table A24.** Applicable power without VVVF inverter for 615 kg during the descent.

| Acceleration Power (kW) | Constant-Speed Power (kW) | Deceleration Power (kW) |
|---|---|---|
| 2.22 | 1.06 | 1.77 |
| 2.24 | 1.02 | 1.79 |
| 2.28 | 1.11 | 1.81 |
| 2.19 | 1.04 | 1.75 |
| 2.16 | 0.99 | 1.73 |
| 2.12 | 0.96 | 1.75 |
| 2.23 | 1.04 | 1.65 |
| 2.25 | 0.97 | 1.69 |
| 2.29 | 0.94 | 1.66 |
| 2.18 | 1.02 | 1.71 |

**Table A25.** Travel time of a lift with VVVF from the ground floor to each floor during ascent and descent.

| Ground | Time Ascent (s) | Time Descent (s) |
|---|---|---|
| 1st Floor | 8.60 | 8.35 |
| 2nd Floor | 11.13 | 10.65 |
| 3rd Floor | 15.20 | 13.65 |
| 4th Floor | 17.73 | 16.65 |
| 5th Floor | 21.03 | 19.65 |
| 6th Floor | 24.33 | 26.65 |

**Table A26.** Travel time of a lift without VVVF from the ground floor to each floor during ascent and descent.

| Ground | Time Ascent (s) | Time Descent (s) |
|---|---|---|
| 1st Floor | 9.88 | 9.80 |
| 2nd Floor | 12.48 | 12.40 |
| 3rd Floor | 15.88 | 15.80 |
| 4th Floor | 19.28 | 19.20 |
| 5th Floor | 22.68 | 22.60 |
| 6th Floor | 26.08 | 26.00 |

**Table A27.** Elevator energy consumption when in standby with VVVF driving and without VVVF inverter for each case.

| Energy Consumption (Wh) | With VVVF Inverter | Without VVVF Inverter |
|---|---|---|
| Scenario 1 | 5336 | 4957.90 |
| Scenario 2 | 5394 | 4992.30 |

**Table A28.** Total area and efficiency of the drive system for each movement of the elevator with VVVF inverter and without driving VVVF inverter.

| Load (Kg) | Total Area (m) | Efficiency Driving System |
|---|---|---|
| 0 Kg with VVVF during the ascent | 1.18 | 72.92% |
| | 3.30 | 30.12% |
| | 1.33 | 96.56% |
| 300 Kg with VVVF during the ascent | 1.18 | 30.19% |
| | 3.30 | 48.24% |
| | 1.33 | 31.06% |
| 615 Kg with VVVF during the ascent | 1.18 | 88.14% |
| | 3.30 | 76.64% |
| | 1.33 | 71.91% |
| 0 Kg with VVVF during the descent | 1.23 | 69.61% |
| | 3.00 | 57.22% |
| | 1.30 | 63.51% |
| 300 Kg with VVVF during the descent | 1.23 | 30.26% |
| | 3.00 | 39.24% |
| | 1.30 | 30.91% |
| 615 Kg with VVVF during the descent | 1.23 | 95.10% |
| | 3.00 | 23.37% |
| | 1.30 | 84.74% |
| 0 Kg without VVVF during the ascent | 1.05 | 64.37% |
| | 3.74 | 38.31% |
| | 2.19 | 77.25% |
| 300 Kg without VVVF during the ascent | 1.05 | 23.54% |
| | 3.74 | 40.46% |
| | 2.19 | 24.52% |

**Table A28.** *Cont*.

| Load (Kg) | Total Area (m) | Efficiency Driving System |
|---|---|---|
| 615 Kg without VVVF during the ascent | 1.05<br>3.74<br>2.19 | 83.60%<br>77.81%<br>68.12% |
| 0 Kg without VVVF during the descent | 1.30<br>3.74<br>1.90 | 76.64%<br>57.51%<br>59.42% |
| 300 Kg without VVVF during the descent | 1.30<br>3.74<br>1.90 | 25.59%<br>35.97%<br>26.75% |
| 615 Kg without VVVF during the descent | 1.30<br>3.74<br>1.90 | 83.60%<br>63.69%<br>94.00% |

**Table A29.** Categories of energy demand in motion.

| Specific Consumption (mWh/mkg) | Category |
|---|---|
| ≤0.8 | A |
| ≤1.2 | B |
| ≤1.8 | C |
| ≤2.7 | D |
| ≤4.0 | E |
| ≤6.0 | F |
| >6.0 | G |

**Table A30.** Categories of energy demand for standby.

| Efficiency (W) | Category |
|---|---|
| ≤50 | A |
| ≤100 | B |
| ≤200 | C |
| ≤400 | D |
| ≤800 | E |
| ≤1600 | F |
| >1600 | G |

**Table A31.** Use categories for lifts according to VDI 4707.

| Use Category | 1 | 2 | 3 | 4 |
|---|---|---|---|---|
| Intensity/Frequency of Use | Low/Rare | Middle/Occasionally | High/Often | Very high/Very Often |
| Average traffic time in hours per day | 0.5 (≤1) | 1.5 (>1–2) | 3 (>2–4.5) | 6 (>4.5) |
| Average waiting time in hours per day | 23.5 | 22.5 | 21.0 | 18.0 |

**Table A32.** Energy-efficiency categories.

| Energy-Efficiency Category | Use Category | | | |
|---|---|---|---|---|
| | 1 | 2 | 3 | 4 |
| A | ≤1.45 | ≤1.01 | ≤0.90 | ≤0.84 |
| B | ≤2.51 | ≤1.62 | ≤1.39 | ≤1.28 |
| C | ≤4.41 | ≤2.63 | ≤2.19 | ≤1.97 |
| D | ≤7.92 | ≤4.37 | ≤3.48 | ≤3.04 |
| E | ≤14.41 | ≤7.33 | ≤5.56 | ≤4.67 |
| F | ≤26.88 | ≤12.67 | ≤9.11 | ≤7.33 |
| G | >26.88 | >12.67 | >9.11 | >7.33 |

## References


1. Skrabulakova, E.F.; Ivanova, M.; Rosova, A.; Gresova, E.; Sofranko, M.; Ferencz, V. On Electromobility and the Calculation of the Infrastructural Country Electromobility Coefficient. *Energies* **2021**, *9*, 222. [CrossRef]
2. Osama, M.; Abdul_Azim, O. Implementation and performance analysis of an elevator electric motor drive system. In Proceedings of the 2008 12th International Middle-East Power System Conference, Aswan, Egypt, 12–15 March 2008; pp. 114–118.
3. Sahu, T.K.; Srivastava, S.; Kushwaha, V.; Aswani, G. Time Optimization of Elevator System using Microcontroller. In Proceedings of the 2020 2nd International Conference on Advances in Computing, Communication Control and Networking (ICACCCN), Greater Noida, India, 18–19 December 2020; pp. 469–471.
4. Plangklang, B.; Kantawong, S.; Dangeanm, S.; Kumsuwan, Y. Elevator Energy Regenerative Unit (EERU) for energy saving in a Permanent Magnet Motor Elevator system. In Proceedings of the 2014 17th International Conference on Electrical Machines and Systems (ICEMS), Hangzhou, China, 22–25 October 2014; pp. 2120–2124.
5. Lee, K.; Ahmed, S.; Lukic, S.M. Universal Restart Strategy for High-Inertia Scalar-Controlled PMSM Drives. *IEEE Trans. Ind. Appl.* **2016**, *52*, 4001–4009. [CrossRef]
6. Khalid, M.; Mohan, A.; Binojkumar, A.C. Performance Analysis of Vectror controlled PMSM Drive modulated with Sinusoidal PWM and Space Vector PWM. In Proceedings of the 2020 IEEE International Power and Renewable Energy Conference, Karunagappally, India, 30 October–1 November 2020.
7. Thu, M.M.; Naing, T.L. α-β Reference Frame Modeling and Implementation of VVVF Three-phase Inverter for Induction Motor Drive. In Proceedings of the 12th National Conference on Science and Engineering (NCSE) 2019, Mandalay, Myanmar, 21 June 2019; pp. 371–376.
8. Ambhorkar, k.; Rana, A.K.; Tutakne, D.R. Enhancing Power Factor and Efficiency of Three Phase Induction Motor Drive using Single Main PWM Switch and Three Auxiliary Swithes. In Proceedings of the 2018 IEEE International Conference on Power Electronics, Drives and Energy Systems (PEDES), Chennai, India, 18–21 December 2018.
9. El Shewy, H.M.; Abd Al Kader, F.E.; El Kholy, M.M.; El Shahat, A. Dynamic Model of Permanent Magnet Synchronous Motor Using MATLAB-Simulink. In Proceedings of the International Conference on Electrical Engineering, Cairo, Egypt, 27–29 May 2008; pp. 1–6.
10. Basera, A.S.; Vora, D.R.; El Kholy, M.M. Variable frequency start of PMSM motor based on STM32f407. In Proceedings of the of 2018 2nd International Conference on Inventive Systems and Control (ICISC), Coimbatore, India, 19–20 January 2018; pp. 191–196.
11. Wu, C.Z. Design of Electrical Control System Elevator Based on VVVF. In Proceedings of the 2015 International Conference on Computational Intelligence and Communication Networks (CICN), Jabalpur, India, 12–14 December 2015; pp. 1490–1492.
12. Karakatsanis, T.S. Modeling of elevators as Driving systems. In Proceedings of the International Association of Elevator Engineering (IAEE), Thessaloniki, Greece, 11–13 June 2008.
13. Bida, V.M.; Samakhvalov, D.V.; Al-Mahturi, F.S. PMSM vector control techniques-A survey. In Proceedings of the 2018 IEEE International Conference of Russian Young Researches in Electrical and Electronic Engineering (EIConRus), Moscow and St. Petersburg, Russia, 29 January–1 February 2018; pp. 577–581.
14. Apte, A.; Walambe, R.; Joshi, V.; Rathod, K.; Kolhe, J. Simulation of a permanent magnet synchronous motor using Matlab-Simulink. In Proceedings of the 2014 Annual IEEE India Conference (INDICON), Pune, India, 11–13 December 2014.
15. Petri, A.M.; Petreus, D. Vector Control of Permanent Magnet Synchronous Motor. In Proceedings of the 2020 IEEE 26th International Symposium for Design and Technology in Electronic Packaging (SIITME), Pitesti, Romania, 21–24 October 2020; pp. 390–393.
16. Sakti, P.S.B.; Riyadi, S. Hardware Implementation of Simplified VVVF Inverter for Induction Motor Based on SVM. In Proceedings of the 2019 International Seminar on Application for Technology of Information and Communication (iSemantic), Semarang, Indonesia, 21–22 September 2019; pp. 487–491.
17. Al-Sharif, L. Variable Speed Drives in Lift Systems. *Elev. Word* **2001**, *49*, 96–106.
18. Pavlova, Y.V.; Grigorii, B.V. The synthesis of a control system of the active rectifier. In Proceedings of the 2018 IEEE Conference of Russian Young Researches in Electrical and Electronic Engineering (EIConRus), Moscow and St. Petersburg, Russia, 29 January 2018–1 February 2018; pp. 941–944.
19. Othman, S.A.; Mohammed, J.A.K.; Mahel, F. Variable Speed Drives in Electric Elevator Systems: A Review. *J. Phys. Conf. Ser.* **2021**, *1973*, 012028. [CrossRef]
20. Li, B.; Wang, C. Comparative analysis on PMSM control system based on SPWM and SVPWM. In Proceedings of the Chinese Control and Decision Conference (CCDC), Yinchuan, China, 28–30 May 2016; pp. 5071–5075.
21. Pechlivanidou, M.S.C.; Kladas, A.G. Winding Structure Impact On High Speed Permanent Magnet Motor Efficiency. In Proceedings of the International Conference on Electrical Machines (ICEM), Valencia, Spain, 5–8 September 2022; pp. 2283–2289.
22. Kutija, M.; Pravica, L.; Godec, D.; Erica, D. Regenerative Energy Potential of Roped Elevator System-A Case Study. In Proceedings of the 2021 IEEE 19th International Power Electronics and Motion Control Conference (PEMC), Gliwice, Poland, 25–20 April 2021.
23. Erica, D.; Godec, D.; Kutija, M.; Pravica, L.; Pavlic, I. Analysis of Regenerative Cycles and Energy Efficiency of Regenerative Elevators. In Proceedings of the 2021 International Conference on Electrical Drives & Power Electronics (EDPE), Dubrovnik, Croatia, 22–24 September 2021; pp. 212–219.

24. Rajy, N.I.; Islam, M.d.S.; Uddin, A.A. Sinusoidal PWM Signal Generation Technique for Three Phase Voltage Source Inverter with Analog Circuit & Simulation of PWM Inverter for Standalone Load & Micro-grid System. *Int. J. Renew. Energy Res.* **2013**, *3*, 647–658.
25. Al-Kodmany, K. Tall Buildings and Elevators: A Review of Recent Technological Advances. *Buildings* **2015**, *5*, 1070–1104. [CrossRef]
26. Lin, K.Y.; Lian, K.Y. Actual measurement on regenerative elevator drive and energy saving benefits. In Proceedings of the International Automatic Control Conference (CACS), Pingtung, Taiwan, 12–15 November 2017.
27. Pham, T.H.; Prodan, I.; Genon-Catalot, D.; Lefevre, L. Efficient energy management for an elevator system under a constrained optimization framework. In Proceedings of the 2015 9th International Conference on System Theory, Control and Computing (ICSTCC), Cheile Gradistei, Romania, 14–16 October 2015; pp. 613–618.
28. Ronquillo, D.G.D.; Dadios, E.P. Solar-powered lifting mechanism for handpump systems. In Proceedings of the International Conference on Humanoid, Nanotechnology, Information Technology, Communication and Control, Environment and Management (HNICEM), Palawan, Philippines, 12–16 November 2014.
29. Manic, M.; Wijayasekara, D.; Amarasinghe, K.; Rodriguez-Andina, J.J. Building Energy Management Systems: The Age of Intelligent and Adaptive Buildings. *IEEE Ind. Electr. Mag.* **2016**, *10*, 25–39. [CrossRef]
30. Kermani, M.; Shirdare, E.; Abbasi, S.; Parise, G.; Martirano, L. Elevator Regenerative Energy Applications with Ultracapacitor and Battery Energy Storage Systems in Complex Buildings. *Energies* **2021**, *14*, 3259. [CrossRef]
31. Pham, T.H.; Lefevre, L.; Genon-Catalot, D.; Pham, V.T. An energy-based control model for autonomous lift. In Proceedings of the IECON 2014—40th Annual Conference of the IEEE Industrial Electronics Society, Dallas, TX, USA, 29 October–1 November 2014; pp. 4286–4292.
32. Sirsi, R.; Kamath, D. Energy Efficient Elevators and Technologies: An Overview. In Proceedings of the 2017 14th IEEE India Council International Conference (INDICON), Roorkee, India, 15–17 December 2017.